Chem Soc Rev

Triggering biological processes: Methods and applications of photocaged peptides and proteins

Journal:	*Chemical Society Reviews*
Manuscript ID	CS-SYN-11-2020-001434.R3
Article Type:	Review Article
Date Submitted by the Author:	24-Jun-2021
Complete List of Authors:	Mangubat-Medina, Alicia; Rice University, Department of Chemistry Ball, Zachary; Rice University, Department of Chemistry

ARTICLE

Triggering biological processes: Methods and applications of photocaged peptides and proteins

Received 00th January 20xx,
Accepted 00th January 20xx

DOI: 10.1039/x0xx00000x

Alicia E. Mangubat-Medina and Zachary T. Ball*

There has been a significant push in recent years to deploy fundamental knowledge and methods of photochemistry toward biological ends. Photoreactive groups have enabled chemists to activate biological function using the concept of photocaging. By granting spatiotemporal control over protein activation, these photocaging methods are fundamental in understanding biological processes. Peptides and proteins are an important group of photocaging targets that present conceptual and technical challenges, requiring precise chemoselectivity in complex polyfunctional environments. This review focuses on recent advances in photocaging techniques and methodologies, as well as their use in living systems. Photocaging methods include genetic and chemical approaches that require a deep understanding of structure-function relationships based on subtle changes in primary structure. Successful implementation of these ideas can shed light on importnat spatiotemporal aspects of living systems.

1. Introduction

Light—or electromagnetic radiation—is perhaps the most powerful external stimulus to probe or alter the internal state of complex biological environments, including cells, tissues, and whole animals. It can be instantaneously delivered from afar with high spatial and temporal control and often with minimal damage to biological systems when using light of suitable wavelengths. Most biological molecules and structures of interest are transparent to light, and some biological pathways have been engineered to respond to or utilize visible light.[1–6] Photocaged peptides and proteins represent one important tool in the toolbox of methods to build light-responsive complex systems.[7–11] Photocontrol has also been accomplished with photoswitches where irradiation with light induces conformational change, though these will not be described in this review.[12–23] Photocaged structures are used to mask enzymatic activity, binding sites, supramolecular assembly, or unique other reactivity that is revealed upon exposure to electromagnetic radiation.[24] In recent decades, photocaging techniques have allowed the discovery and study of important, complex biological pathways and mechanisms. Spatiotemporal control of specific individual molecule activation, made possible by photocaging concepts, has proven to be a remarkably empowering capability.

Photocaging concepts are often akin to photocleavable protecting groups in small-molecule and polymer chemistry.[24,25] Irradiation with light induces selective bond scission, releasing a product with native structure or with some other desirable biological activity. There is an ever-increasing need to develop photocaging concepts and the chemical methods to synthesize caged structures. Among the challenges that drive this innovation are the diverse structures and functional groups found in biological systems, the need for multiple orthogonal photo-uncaging regimes, and the difficulties of tissue penetration. Furthermore, the complexities of predicting reactivity in complex environments based on much simpler small-molecule models tend to necessitate a variety of complementary photocaging approaches.

Since the landmark photocaging of adenosine triphosphate (ATP) in 1978,[26] a range of photocaged small molecules has been reported, allowing light-triggered perturbation of biological systems.[11] More recently, a variety of photocaged biomacromolecules (such as peptides, proteins, DNA,[27–30] and RNA[31–36]), bioactive small molecules,[1,2,37–46] and bio-compatible polymers[47–49] have appeared, bringing a new set of tools to bear on biological problems. The relative paucity of early examples of photocaged peptides and proteins reflects the synthetic and analytical challenges to implementing a clean and predictable photo-uncaging concept. In this review, we examine the diverse approaches to construct photocaged peptides and proteins, focusing on recent advances. We focus on the chemical and synthetic challenges of accessing these photocaged structures, and present representative examples of the biological applications that demonstrate current capabilities and future potential of these discoveries.

Photocaging groups that unmask natural structure via bond scission incorporate diverse core structures, such as 2-nitrobenzyl (**1**-**3**, Figure 1), bromonitroindoline (**4**),[50–52] benzoin (**5**),[53–56] bimane (**6**),[57,58] coumarin (**7**-**15**),[59–65] and nitrodibenzofuran (**17-19**).[66,67] This structural diversity is important to the goal of obtaining structures with diverse wavelengths of uncaging reactivity. The 2-nitrobenzyl core, one of the most widely used, was first described in 1966[68] and has

[a] Department of Chemistry, Rice University, Houston, TX, 77005, United States.

been used to cage cysteine (Cys),[67,69–75] serine (Ser),[76] tyrosine (Tyr),[77,78] aspartate (Asp),[79] glutamate (Glu),[80,81] asparagine (Asn),[82] glutamine (Gln),[83] and lysine (Lys)[73,84,85] residues. Other photocaging agents have been less commonly employed, often with demonstrated utility with a much smaller subset of this group. Broadly speaking, photocaging has been demonstrated with nearly all the polar or charged amino acids, while photocaging nonpolar amino acids is relatively unexplored.

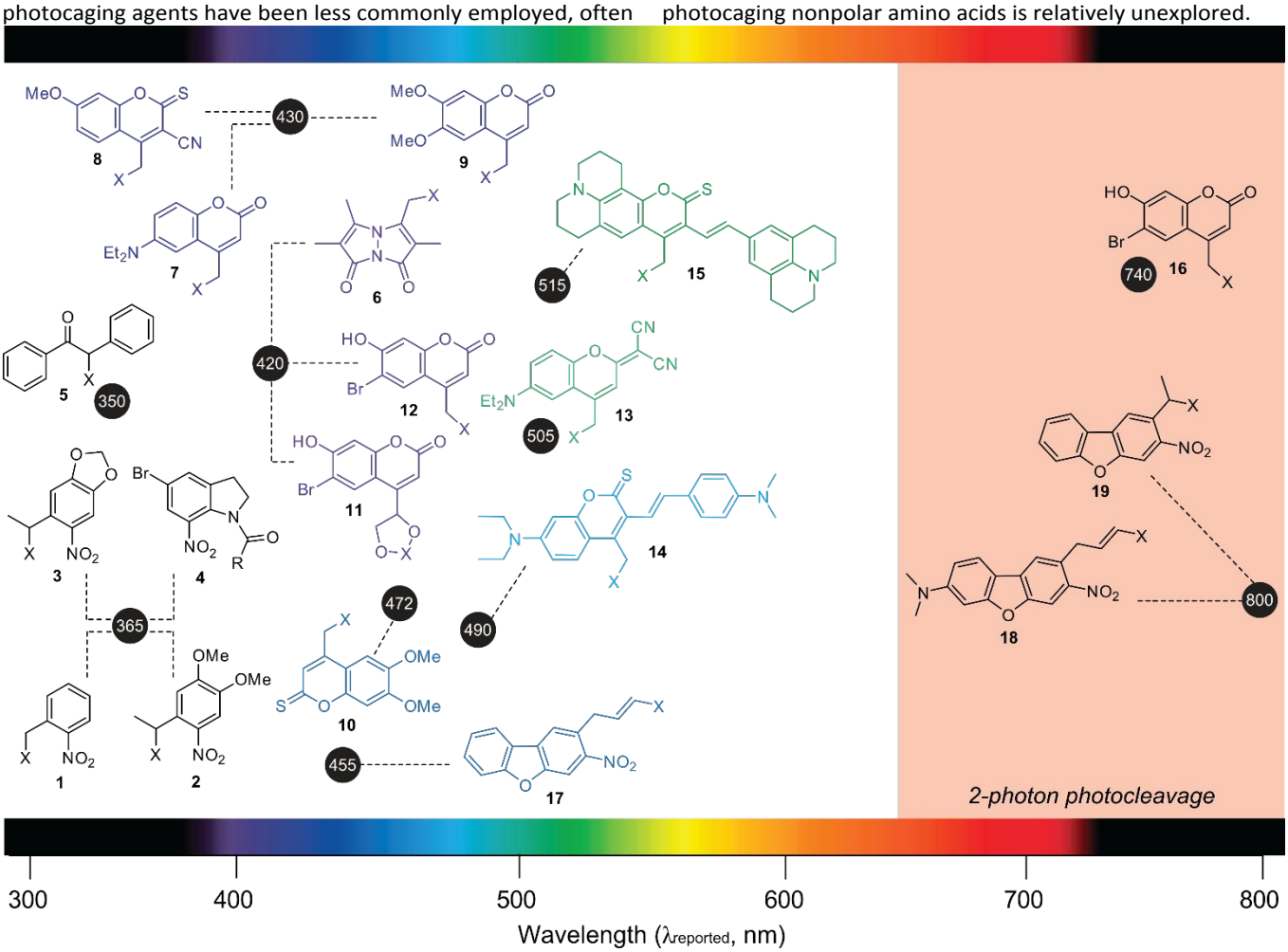

Figure 1. Photocaging groups and their reported wavelength of photocleavage[50-67] where (X) is the photocaged functional group.

Current photocaging reactions have mechanistic aspects in common. In one such example, the nitrobenzyl group (Figure 2, **A**) undergoes a photoreaction when irradiated with UV light via a C–H abstraction (Figure 2, **B**) mechanism leading to sp^3 C–X bond cleavage (Figure 2, **E**), and many other photocaging agents follow suit. This is probably the primary reason that side-chain photocaging has been limited to polar (heteroatom-containing) amino acids, although limited approaches to photocaging backbone N–H bonds provides an alternative photocaging at such residues.[86–88] Coumarin, for example, has been used to photocage the side chain of Cys,[89] Lys,[90] and the C-terminus of glycine (Gly),[64] setting the stage for a structurally similar photocleavage of a (hetero)benzylic C–X bond that occurs by a rather different photochemical heterolytic C–X cleavage mechanism.[63,91,92]

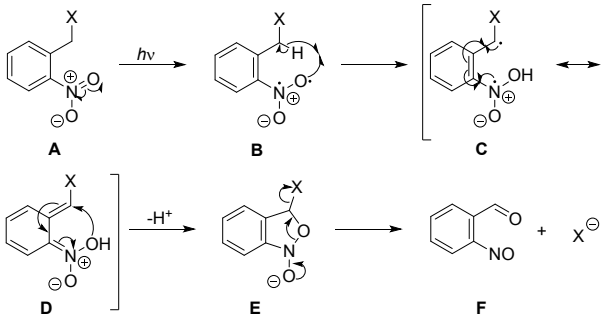

Figure 2. Nitrobenzene uncaging mechanism.

Designing photocaging structures has lagged behind that of analogous light-emitting compounds, such as fluorophores.[93,94] Quantitative data for cleavage efficiency remains limited, and even complete understanding of effective cleavage wavelengths is sometimes lacking (Figure 1). Effective uncaging at wavelengths above 450 nm is quite limited. Efficient cleavage of nitrobenzyl chromophores are typically limited to ultraviolet or blue wavelengths (<365 nm), and many alternative structures

have similar limitations. A few structures (e.g. **13, 15, 16-19**) have been shown to cleave above 500 nm, and some efforts to develop orthogonal pairs of cages with different uncaging wavelengths have been made.[62] But full understanding of capabilities for red-shifted uncaging is still being uncovered. Layered on top of this discussion, there is also significant interest in developing photocaging groups with efficient two-photon activation, which would allow uncaging at near-IR wavelengths (e.g. >700 nm, **16-19**) that are most transparent to living tissue.[67,87,95,96]

Photocaged peptides and proteins have unique capabilities for developing our understanding of biological function. Photocaging a biomacromolecule of interest is a more direct and time-controlled method of controlling function, compared to more roundabout inhibitor- or transcription-based approaches. Despite the potential, synthetic preparation of photocaged peptides and proteins remains challenging. Photocaged peptides are often accessed by variations of solid-phase peptide synthesis (SPPS). Combining SPPS with native chemical ligation concepts also provide access to photocaged proteins, though on a limited basis. Photocaged protein synthesis is also accomplished through genetic incorporation of photocaged unnatural amino acids. This review is divided into two parts: first, the synthetic methods for accessing photocaged peptides and their applications are described, and second, the complementary methods for accessing photocaged proteins and their applications are described.

2. Overview of photocaged amino acids for peptide and protein synthesis

Photocaged polypeptides have uniformly relied on C–X bond cleavage to reveal natural functionality. This typically means photocaging via a cleavable C–O bond (Ser, Tyr, Asp, Glu), C–N bond (Lys, Asn, Gln, N-terminus), or C–S bond (Cys). Thus, photocaging has typically been limited to polar or charged side chains. In broad terms, typical photoprotecting groups are general, and the same group could be used to photocage a variety of side chain structures. Indeed, the 2-nitrobenzyl group and its derivatives has been used to cage many different side chains, including Cys,[67,69–71,74,95–97] Ser,[76,98] Tyr,[99] Glu,[100] Asp,[100–102] and Lys.[84,90,103] A common alternative to the 2-nitrobenzyl group is coumarin and its derivatives which was used to photocage Cys, Lys, and Asp. However, it must be noted that these photocaging groups all require UV light to uncage their substrate, save for rare examples of two-photon sensitive photocages and a single example of a green-light sensitive photocaged Asp, well above the wavelength range accessible with most photocleavage structures.[102] Even in those cases with two-photon sensitivities, photocleavage is generally more efficient in biological contexts when irradiated with UV light.[67]

Recombinant incorporation of photocaged unnatural amino acids (UAAs) via a unique tRNA is an important method for incorporating photocaged amino acids. An impressive array of photocaged residues has been accessed by UAA technologies, including Lys, Tyr, Ser, and Cys,[74,99,104] although it is probably fair to say that recombinant methods remain structurally more limited than chemical approaches. Of these, photocaged Lys is perhaps the best-studied case, due to the ease of utilizing and/or evolving natural pyrrolysine processes. Indeed, even wavelength limitations have been addressed for Lys, with one example demonstrating two-photon uncaging above 700 nm.[90]

3. Photocaged peptides: synthesis and applications

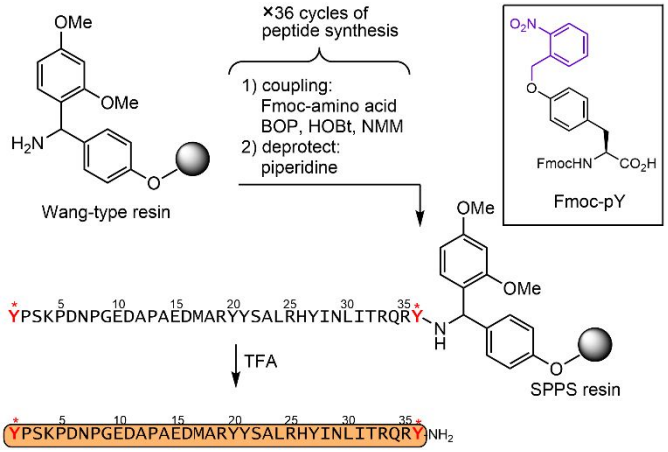

Figure 3. Fmoc-based synthesis of a 36-mer peptide with photocaged lysine residue(s). Incorporation of a photocaged tyrosine derivative at position Y1 and/or Y36 was accomplished with the reagent Fmoc-pY.

3.1 Synthesis of photocaged peptides

Synthetic access to photocaged polypeptides is often more straightforward than that for photocaged proteins, due to the flexibility of solid-phase peptide synthesis (SPPS). However, there are at least three approaches to introduce photocaging groups into peptides: (i) solid-phase peptide synthesis using a photocaged amino acid (pAA), (ii) solid-phase, functional-group-selective reaction to install a photocaging group, and (iii) solution phase modification of a natural amino acid sequence.

3.1.1 SPPS using unnatural amino acids

Side-chain photocaged amino acids: The reliability and broad applicability of modern peptide synthesis methods has meant that installation of diverse side-chain photocaging groups within diverse peptide sequences is often possible without the need for special optimization or method development. While Boc solid-phase synthesis has important benefits in select applications,[105] Fmoc solid-phase synthesis has become "the method of choice for peptide synthesis,"[106] and this is reflected in the literature of photocaged peptides as well. We are not aware of any reported examples of Boc solid-phase synthesis to access photocaged peptides, but Fmoc solid-phase synthesis of these targets is common.

Thus, compatibility with standard Fmoc SPPS techniques is one important factor in choice of photocaging structure. In one early example[107] (Figure 3) caged analogues of the 36-mer neuropeptide Y was synthesized using an BOP/HOBt coupling approach, incorporating photocaged tyrosine residues at one or two tyrosine residues following global deprotection/cleavage with TFA. Notably, the effort required no special modification of

conditions to incorporate the photocaged residues, and this observation is consistent with other reports.[108,109] The incorporation of photocaged tyrosine at both N- and C-terminal residues demonstrates the compatibility with even long synthetic operation. A variety of Fmoc SPPS-compatible structures are in common use. Peptides with photocaged Cys [67,71] Asp,[101,102,100] Glu,[100] Ser,[98] Lys, [108,84,90,110,103] and Tyr[107] have been constructed using standard Wang and Rink Amide resins (Figure 4).

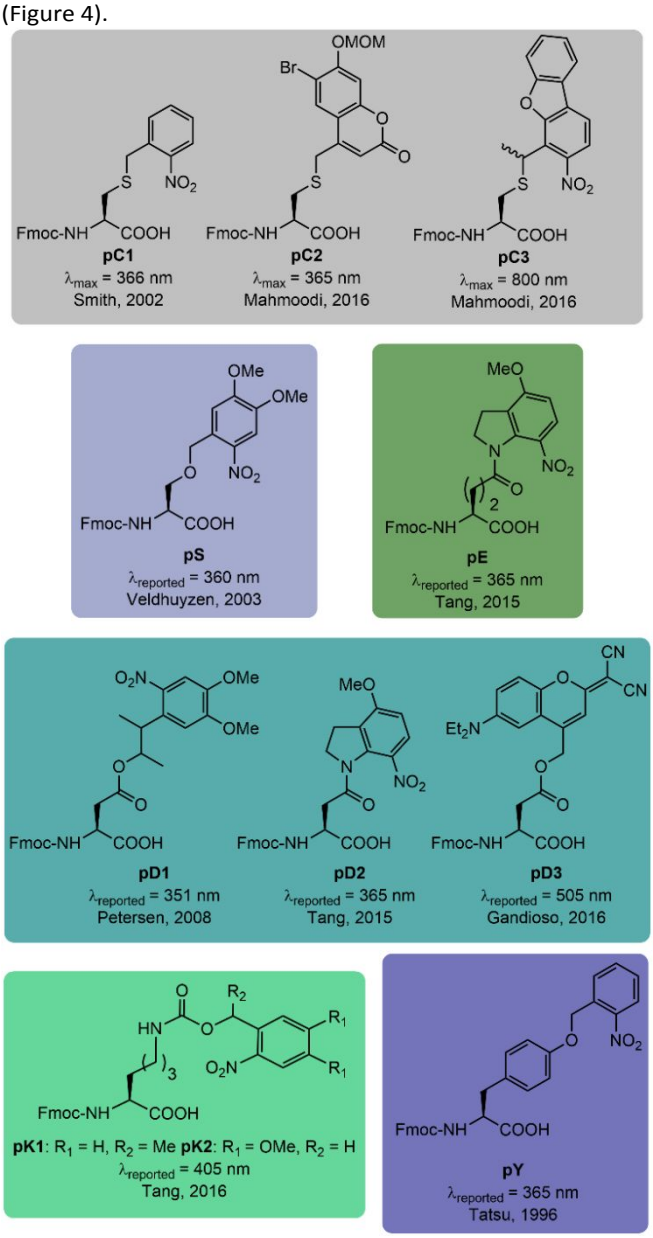

Figure 4. Representative examples of photocaged side-chains that have been shown to be compatible with SPPS. $\lambda_{reported}$ is the wavelength of photocleave reported in the cited literature.

The lion's share of examples to date involves photocaging of side-chain functional groups. Photocaged side chains are similar enough to traditional side-chain protecting groups in SPPS that the photocaged amino acid can be treated just as any traditional amino acid in routine peptide synthesis. However, the N-terminus, C-terminus, or even specific backbone amide bonds are all potentially valuable alternative photocaging sites that may require unique synthetic approaches.

The essential role of backbone H-bonding in secondary structures, such as α-helices or β-sheets, makes backbone amide photocaging an intriguing tool to directly control folding, structure, and function with light. But unlike side chain photocaging, access to sequences with modifications of backbone structure requires creative synthetic approaches. Peptides photocaged at backbone Gly N–H bonds have been synthesized by solid-phase synthesis,[111] producing, for example, photocaged analogues of collagen-mimetic peptides[112] and amyloid peptides.[88] Incorporation of *N*-(2-nitrobenzyl)glycine (Figure 5, path 1A) directly was found to be practical within unhindered Gly-Gly-Gly triads, and subsequent coupling of the secondary amine (path 1B) could be accomplished with DIC.[111] To access other sequences, a corresponding two-step approach with bromoacetate coupling followed by amine alkylation was developed (Figure 5, path 2A),[88] and the subsequent coupling of the secondary amine (path 2B) required the strong activating agent, triphosgene.[88] However, the generality of both approaches is limited by poor coupling efficiency of the secondary amine in the photocaged monomer. No examples extending these concepts to amino acids other than Gly have appeared, presumably due to the steric demands of α-branching, and even photocaged Gly (Figure 5) is a synthetic challenge. Typical carbodiimide coupling agents, and even modern highly effective coupling reagents such as HATU, fail to deliver effective coupling in sterically demanding situations.

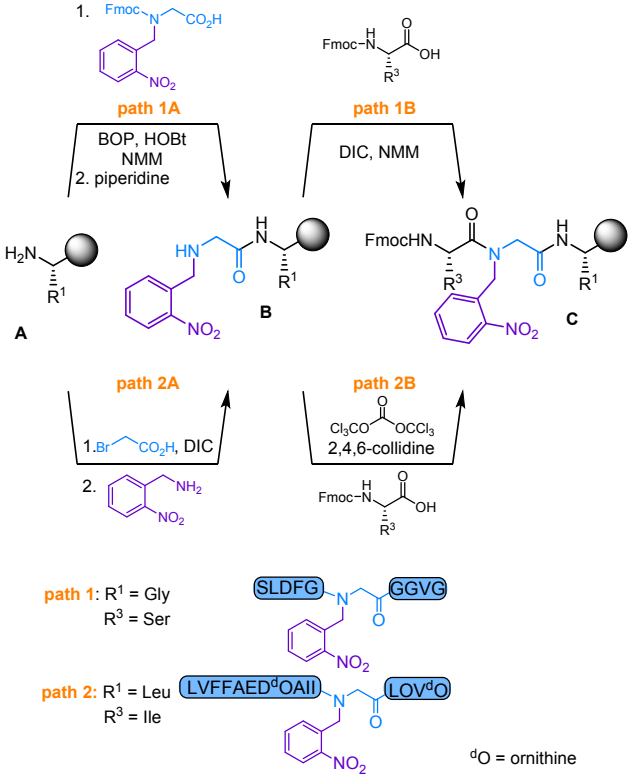

Figure 5. Examples of installing photocages on backbone structures through SPPS. (Path 1) Photocaged Gly within a G**G**G sequence could be introduced as an *N*-benzyl amino acid with minor adaptation of standard coupling reagents. (Path 2) Within a more hindered sequence, photocaged Gly was introduced by an alkylative approach (path 2A), and the subsequence coupling required triphosgene (path 2B).

3.1.2 Solid-phase selective functional group photocaging

Site-specific photocaging can also be accomplished through a unique, orthogonal protecting group. In this case, selective mono-deprotection allows installation of a photocaging agent prior to global deprotection and release from resin. This approach is valuable in cases where a chemically sensitive photocaging agent is desired. Diederichsen *et al*. demonstrated selective N-terminal modification, on-resin, to install a photocleavable auxiliary for photoactivated native chemical ligation (NCL).[113] This N-terminal photocage was synthesized as a nitrobenzyl derivative and installed onto the peptide by reductive amination (Figure 6). A variation of NCL[113] with N-terminal photocleavable auxiliaries has been used to ligate peptide fragments, forming a larger target peptide with a photocleavable group at a specific backbone N–H bond. An initial report (Figure 6) demonstrated ligation through a pathway involving trans-thioesterification and an S→N acyl shift. The unhindered Gly-Gly and Ala-Gly gave 14-mer peptide products in good yield, while attempts to form more hindered linkages, such as Gly-Leu, gave significantly diminished yields. As a method for the preparation of large native peptides, significant improvement in the method would be needed to make the process effective and general for preparative use, and in cellulo or in vivo applications of this concept have not been reported. However, the concepts outlined here could be valuable for unique applications targeting structures not accessible by genetic (unnatural amino acid) approaches.

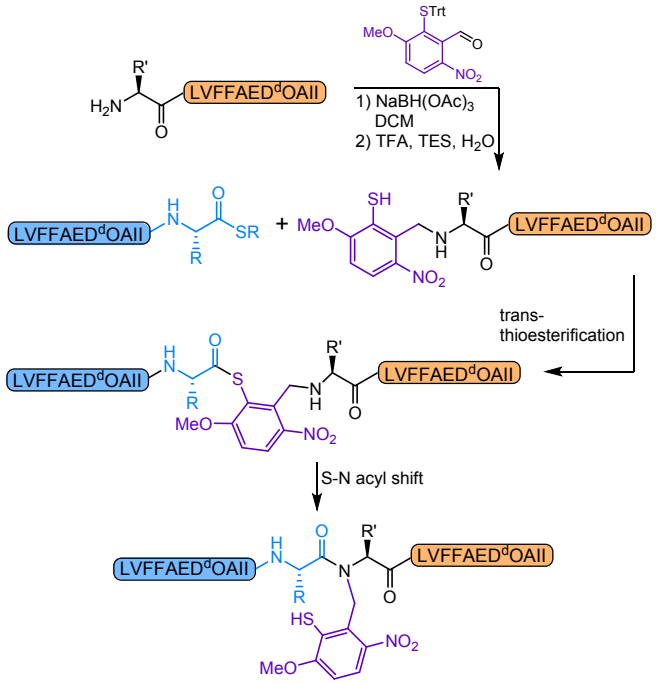

Figure 6. Photocleavable auxiliary allows NCL to occur at sequence sites without Cys.

3.1.3 Solution-phase selective functional group photocaging

The major alternative to incorporating photocaging agents during SPPS is selective solution-phase reactions on polypeptides. Solution-phase methods may be especially desirable for peptides isolated from whole organisms or otherwise biological in origin. In addition, some photocleavable targets may be incompatible with SPPS methods, as is often the case with C-terminal photocaging structures.[114] In fact, the first on-resin C-terminal photocaging was described by So and Xia in 2020 using a three-component Passerini reaction.[115] On the other hand, solution-phase modifications of peptides create the reactivity and selectivity challenges typical of selective reaction design in complex polyfunctional environments. Ideal solution-phase methods might permit photocaging of fully unprotected sequences, but in practice selectivity concerns often require rather complex protecting-group strategies.

In an early example of selective solution-phase photocaging, a photo-reactive guanylating agent was reacted with an ornithine side chain of a peptide inhibitor of the cAMP-dependent protein kinase (PKA) to form photocaged arginine (Arg) (Figure 7). This photocaged Arg allowed photocontrol of cAMP signaling.[116] The group used Fmoc protection of the N-terminus, retained from SPPS, to avoid competing reactivity. The creation of a caged Arg structure with this method is straightforward and efficient, but the chemistry required anhydrous conditions (DMF), and orthogonal protection of amine groups, limiting the utility of the approach. Many other examples of solution-phase photocaging similarly require sophisticated protecting-group strategies and organic-phase reaction conditions. C-terminal amidation or N-terminal carbamate formation reactions, for example commonly involve coupling reagents such as HCTU[117] or TBTU,[114] respectively.

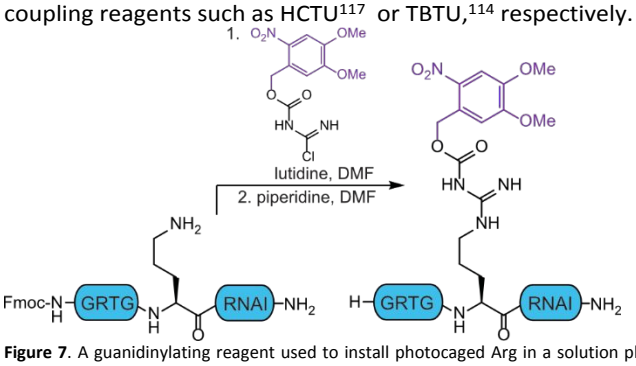

Figure 7. A guanidinylating reagent used to install photocaged Arg in a solution phase procedure that required orthogonal protection of other amino groups.

While photocaging most commonly masks a specific functional group, photocleavable stapling ideas have been advanced as a way to use topological constraints to alter peptide function (Figure 8).[114] Olefin metathesis was employed as a key method to cyclize (or "staple") a small peptide after stepwise installation of two terminal olefins via typical amidation and carbamate formation methods. Photocleavage of both linkers then permits traceless release of the parent linear peptide. It is important to note, that examples described contain only hydrocarbon side chains, obviating the need for protecting groups.

Relatively few studies provide approaches to photocaging non-protected polypeptides with diverse side chains. Copper-catalyzed, histidine-directed coupling of boronic acids with a specific backbone N–H bond was shown to occur in water with fully deprotected peptide substrates (Figure 9).[118] Molecular design of a light-sensitive alkenylboronic acid (Figure 9, **B**) reagent allowed preparation of photocleavable backbone

conjugates, creating a 1-step approach to specific backbone photocaging governed by a neighboring histidine (His) residue (Figure 9).[86] The design hinges on a vinylogous analogue of 2-nitrobenzyl photocaging agents (i.e. Figure 2). The photocleavage of an alkenyl–X bond in this instance is noteworthy.

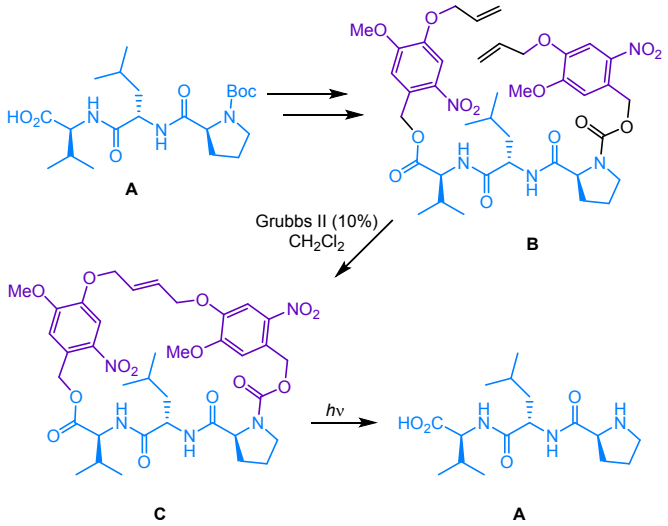

Figure 8. Two photocaging groups, covalently linked by an olefin metathesis reaction with the Grubbs II catalyst, provide a topologically constrained cyclic peptide **C**, which releases the parent linear peptide **A** upon irradiation.

This photocaging method was used to cage peptidase substrates. Peptidase activity is often highly sensitive to local structure,[119] and alteration with a photocaging group or other bulky group is often sufficient to abrogate activity.[69,120,121] Copper-catalyzed backbone modification of a α-chymotrypsin substrate peptide (CSP) gave compound **C** (Figure 9). Consistent with expectation, photocaged peptide **C** was completely resistant to peptidase activity, while enzymatic proteolysis occurred quickly upon irradiation, affording peptides **D**–**E**. This photocaged peptide concept may be valuable in affording spatiotemporal control of proteolytic processing of pro-hormones in vivo.

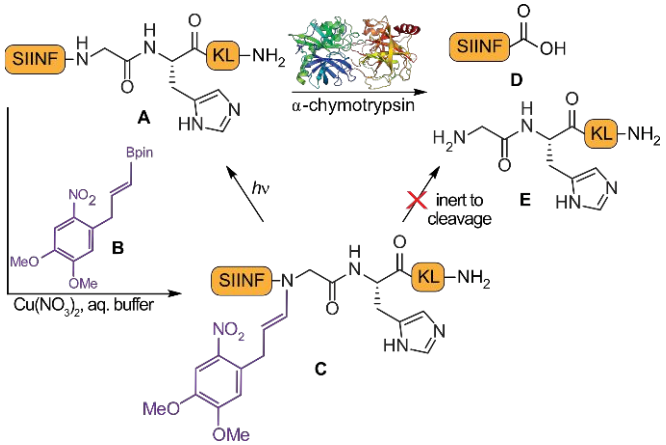

Figure 9. Histidine-directed, Cu^{II}–catalyzed backbone N–H photocaging an α-chymotrypsin cleavage sequence with boronic acid **B**. The N–H alkenylation product **C** is inert to α-chymotrypsin.

3.2 Applications of photocaged peptides

3.2.1 Photocaging RGD peptides for triggered cell patterning

Cell adhesion is mediated by interactions with the short sequence, Arg-Gly-Asp (RGD).[122] This fundamental recognition event is important for artificial scaffolds for tissue engineering[123,124] and controlled cell growth on surfaces,[125] and RGD recognition has important consequences for human medicine.[126] Consequently, controlling RGD-mediated adhesion by light or other external stimulus has received attention.[127–130] Covalent side-chain photocaging allows light to turn on cell adhesion.[80,101] In one such approach, SPPS produced a photocaged RGD peptide with backbone N-alkylation (2-nitrobenzyl) at the key Gly residue which was immobilized on poly-L-lysine.[80] Alkylation effectively blocked activity, and no adhesion was observed for caged peptides attached to a poly-L-lysine surface. Exposure to light liberates the RGD motif, and the expected cell adhesion and spreading was observed. (Figure 10a).

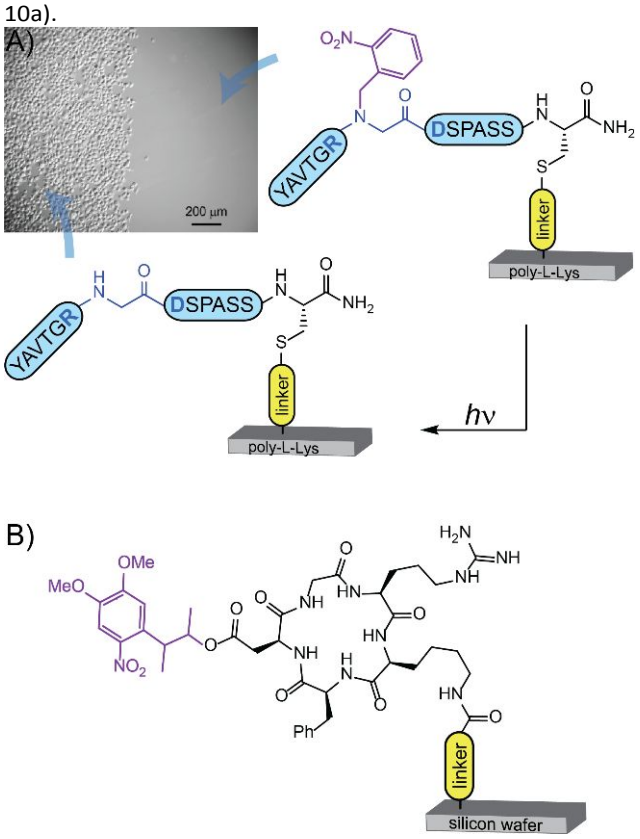

Figure 10. Spatial control of cell adhesion with immobilized photocaged RGD peptides. (a) Photocaged RGD peptides were immobilized on a poly-L-Lys surface and cells adhered to the irradiated left half of the surface. Copyright © 2008 WILEY-VCH Verlag GmbH & Co. KGaA, Weinheim. (b) Photocaged RGD peptides immobilized though a PEG linker to a silicon wafer.

In a complementary approach,[101] installing a photoreactive DMNPB ester[131] at an Asp side chain within a cyclic RGD sequence, again by SPPS, was used to prepare photoactivatable surfaces on silica (Figure 10b). The study also marked an early application of DMNPB esters, which were developed for high cleavage quantum efficiency (irradiation at 351 nm).[131] Similar to the backbone Gly caging, DMNPB esters block key Asp interactions with the integrin MIDAS region,[132] and similar photocontrol of cell surface adhesion was achieved. These two

studies also validate the compatibility of photocaging with surface-immobilized sequences, employing maleimide–cysteine[80] or siloxane–silica[131] immobilization chemistries.

Cis-trans photoisomerization of azobenzene has been employed as a complementary approach to light-controlled RGD recognition. Light-driven cis-trans isomerization can also produce changes in biological function by changing the local structure and steric environment around a ligand, without any bond-breaking. Azobenzene photoisomerization can reversibly "switch on" a new biological state.[133–135] Tethering an RGD peptide to a surface via an azobenzene linker produced a surface in which exposure to light induced isomerization to a cis, non-adhesive state.[136]

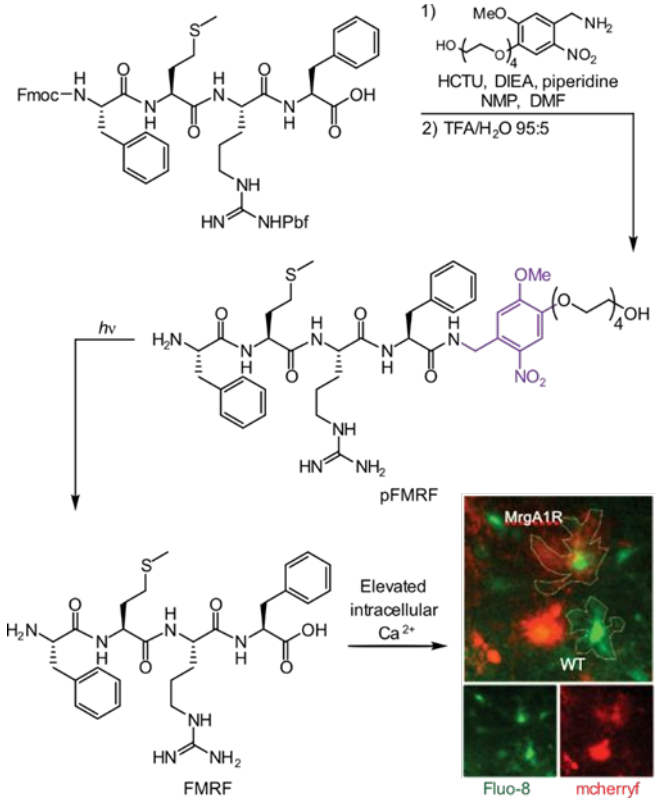

Figure 11. Synthesis of a photocaged agonist peptide (pFMRF). HCTU coupling installs a 2-nitrobenzyl derivative of a C-terminal amide group. Uncaging (hv) produces active agonist peptide (FMRF). (inset) confocal images of astrocytes demonstrating elevated intracellular calcium levels (green, Fluo-8). Areas exposed to 365-nm light (inside white outline) exhibited a spike in Ca^{2+} levels within cells exposed to pFMRF. Reprinted with permission from *Bioconjugate Chem*. 2015, 26, 12, 2408–2418. Copyright 2015 American Chemical Society.

3.2.2 Light-activated investigation of cell-cell interactions

Like cell-surface interactions, cell-cell interactions have been fertile group for photocaged peptide applications. Photocaged peptides offer a unique ability to learn about biological pathways in a time-resolved fashion. In a study by Janett *et al*., a C-terminal photocaged neurotransmitter offered a peek into neuron–glia communication (Figure 11).[117] As the two main classes of neural cells, a clear understanding of the interactions between neurons and glia are critical for understanding brain function.[137,138] Astrocytes, the most abundant of glia cells, can monitor and alter synaptic function and structure, resulting in control of synaptic transmission in the brain.[139] Astrocytic calcium elevation is a key indicator of astrocyte-neuron communication. In one study, a synthetic photocaged agonist peptide, Phe-Met-Arg-Phe (pFMRF), of Mas-Related-Gene Gq-coupled-receptor (MrgA1R) enabled photo-triggered neuronal interactions within astrocytes. Intracellular spikes in calcium levels were readily imaged by confocal microscopy (Figure 11, image).[117] Cells displaying MrgA1R receptors were exposed to the pFMRF agonist, and spikes in intracellular calcium levels were observed, dependent on UV exposure.

3.2.3 Peptide activation within live cells

Controlling peptide activation within cells is an intriguing challenge which lends itself to exploring mechanisms of action within biological contexts. Unlike extracellular activity, intracellular studies require an understanding of cell entry, subcellular compartmentalization, and intracellular protease stability. In one key example, a photocaged Cys was deployed to study enzymatic palmitoylation of peptides.[67] In the report, 2-nitrodibenzofuran was selected as the Cys photocage for its efficient UV- and two-photon-cleavage abilities. Alternative 2-photon sensitive photocages such as brominated hydroxycoumarin were not compatible with Cys photocaging in all contexts due to photoisomer side products upon irradiation, as reported by the authors. The nitrodibenzofuran was installed within K-Ras-derived and Cys-Leu-Cys (CLC) peptides for enzymatic and cell studies, respectively.[67] The CLC peptide was tagged with an NBDhex fluorophore to allow visualization of cellular localization. Cys *S*-palmitoylation induces migration to the membrane, and the photocaging approach allowed direct real-time visualization of palmitoylation and subsequent membrane localization (Figure 12).

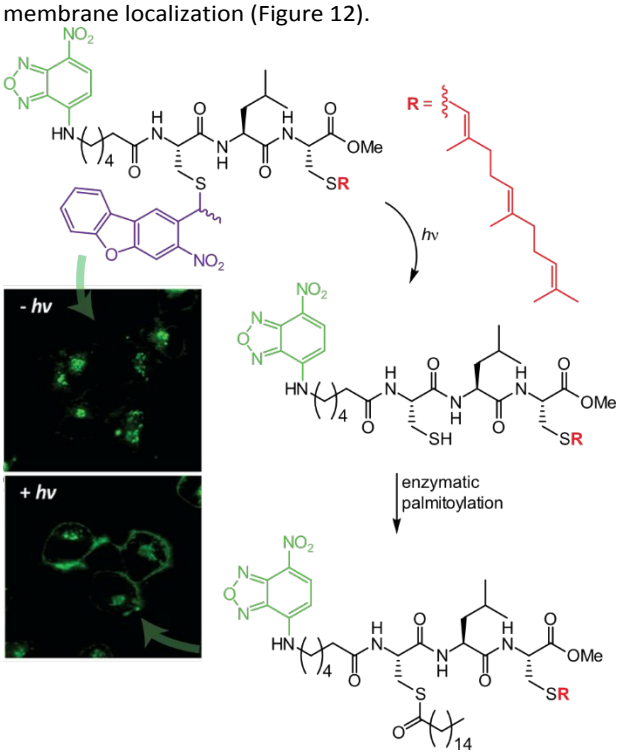

Figure 12. Scheme of NDB-hexCLC peptide uncaging and subsequence palmitoylation. Left: confocal images of peptide migration following irradiation of caged NBD-hexCLC peptide. Cell images reprinted with permission from *J. Am. Chem. Soc.* 138, 18, 5848. Copyright 2016 American Chemical Society.

3.2.4 Probing amyloid oligomers through photocaged peptides

The complicated kinetics, initiation, and speciation of amyloid aggregation are confounding problems tailor-made for a photocaging approach. Chemical means of controlling or initiating amyloid assembly can provide valuable in vitro information. But chemical methods have drawbacks or are impossible in more realistic cellular models of disease, and light-driven release of amyloid sequences has been pursued as a solution to this problem. In one important study, light-induced amyloid fibrillation was observed in neuroblastoma cells (SH-SY5Y) exposed to photocaged Aβ-derived macrocyclic peptides (**peptide NB**, Figure 13).[88] Before irradiation, the photocaged peptides were nontoxic up to 100 μM as measured with MTT assays (Figure 13). Following irradiation, membrane disruption was observed at uncaged peptide concentrations as low as 50 μM. The work indicates the potential for photocaged peptides to deliver and probe the effects of sensitive and/or metastable species in cellular environments.

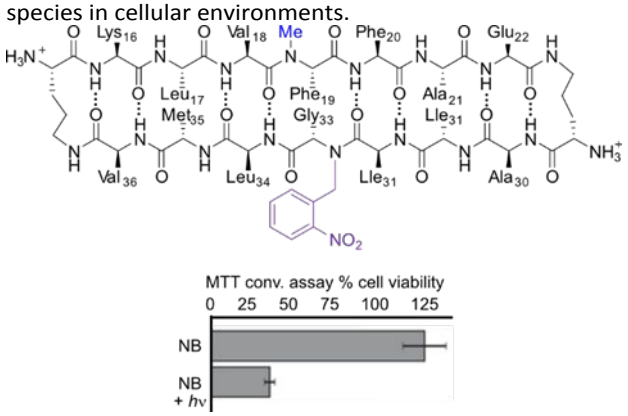

Figure 13. Photocaged Aβ-derived macrocyclic **peptide NB**. MTT conversion assays indicate that only the uncaged form of peptide NB (**peptide NB** + *hν*) cause cell death. Reprinted with permission from *J. Am. Chem. Soc.* 140, 17, 5842. Copyright 2018 American Chemical Society.

3.2.5 Phototriggered collagen mimetic peptide folding

Similarly, collagen sequences are metastable monomers that undergoes spontaneous assembly. Collagen assembles into initial triple helices, which further assemble into a variety of collagen biomaterials.[140,141] Collagen-mimetic peptides (CMP) have been developed to model, mimic, and directly interface with, natural sequences.[142–146] Controlling the kinetics and initiation of aggregation in these systems is important for our fundamental understanding of the assembly processes but is also essential for a range of biomedical or chemical biological applications of CMPs. The two studies of photocaging concepts on collagen systems used SPPS and solution-phase synthesis to install a photocaged backbone N–H at Gly.[86,112] This photocaged CMP exhibited light-induced folding (

Figure **14**a-b) upon exposure to UV light.[86] In further studies, UV light triggered the photocaged CMP sequences to co-assemble with degraded natural collagen in mouse model. Increased matrix metalloproteinase (MMP) activity, which is correlated with several pathogenic conditions, remodels collagen in diseased tissue, producing degraded collagen structures that were visualized by a fluorescently-tagged, photocaged CMP (Figure 14c).[112]

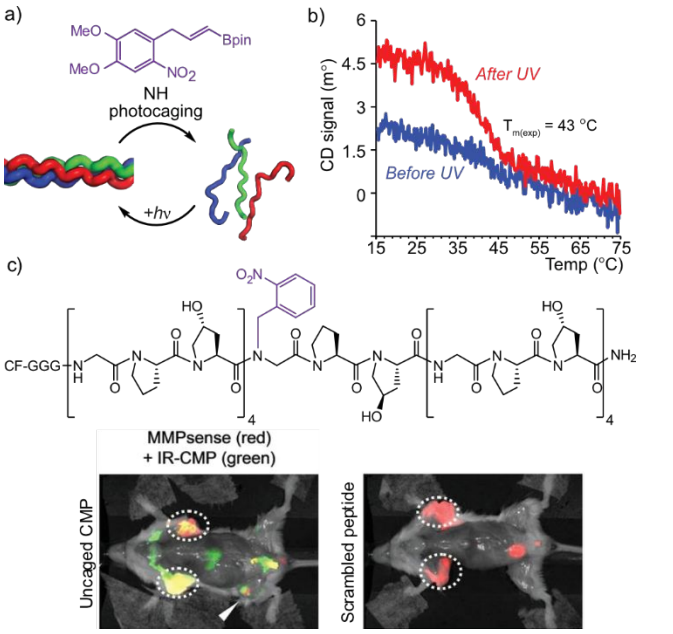

Figure 14. CMP modification-driven unfolding and photocleavage-driven refolding (a). (b) CD melt analysis indicating folding of modified CMP before (blue) and after (red) photocleavage with 365 nm light. Reprinted with permission from *J. Am. Chem. Soc.* 140, 27, 8401. Copyright 2018 American Chemical Society. (c) Photo-triggered triple-helical folding of caged CMPs for detecting MMP activity in mouse models. Reprinted from Ref. 107 with permission from the National Academy of Sciences.

4. Photocaged proteins: synthesis and applications

Proteins, while structurally and functionally similar to peptides, come with a host of additional challenges when photocaging these complex structures. Proteins generally require aqueous conditions, limiting chemical techniques available to photocage these macromolecules. Furthermore, when proteins are modified from their native structure, their behavior and stability are perturbed, leading to tractability problems. While peptides have a whole host of photocaging technologies, such techniques for proteins are, in comparison, quite limited. Here, the synthetic technologies for photocaging proteins and applications of these photocaged proteins are described.

4.1 Synthesis of photocaged proteins

4.1.2 Genetic encoding of pAAs

Genetic encoding of photocaged amino acids (pAA) in whole proteins is now well established. Multiple reviews[147–152] cover the topic of photocaged UAA incorporation extensively, and readers interested in a thorough treatment of that subject are directed there. In brief, an unnatural tRNA charged with the caged UAA is used to insert the UAA at a specific codon, typically a stop codon. Evolution of an orthogonal tRNA synthetase allows effective UAA incorporation in vivo. This review provides an overview of the scope of photocaged UAAs and focuses on unique approaches involving novel chemistries. In 1998, a genetic incorporation of a photocaged Tyr by nonsense/stop codon suppression technology was reported,[77] and in subsequent years genetic incorporation of photocaged side

chains has proven broadly useful.[97,99,104,149,153–161] Using a nonsense anticodon tRNA modified with the photocaged Tyr (**pY**, Figure 15), the muscle nicotinic acetylcholine receptor (nAChR) containing a photocaged Tyr in the α subunit was expressed in *Xenopus* oocytes.[77] Building on prior work to incorporate UAAs in nAChR,[162–164] both unnatural tRNA and mRNA encoding the desired nAChR protein were microinjected into oocytes. Other early examples include the incorporation of photocaged Cys (**pC1**) by the Schultz group, where *E. coli* leucyl tRNA synthetases were evolved by randomizing the amino acids (Met40, Leu41, Tyr499, Tyr527, and His537) that form the hydrophobic pocket, based on suppression of stop codons at positions 44 and 110 in the *gal4* gene.[74] Since this first report, many efforts have utilized such mutant pairs of *E. coli* leucyl-tRNA synthetase (EcLeuRS)/tRNA and pyrrolysyl-tRNA synthetase (PylRS)/tRNA in yeast and mammalian cells for the genetic encoding of pAAs.[148,165]

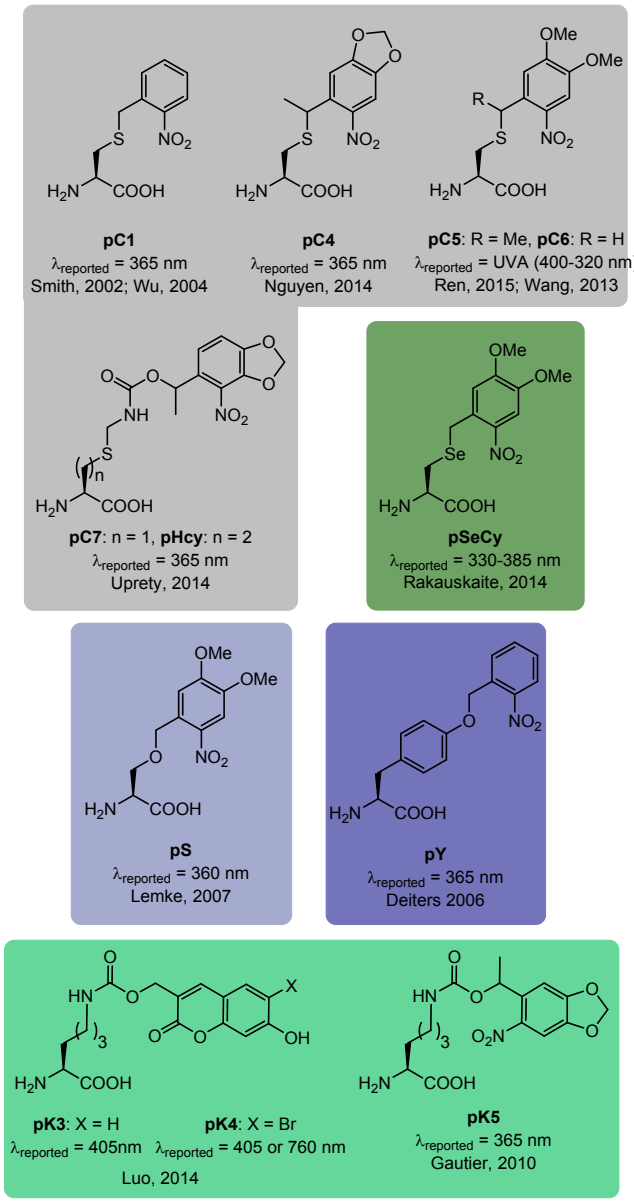

Figure 15. Genetically incorporated photocaged amino acids. $\lambda_{reported}$ is the wavelength of photocleave reported in the cited literature.

This technology has now expanded significantly: tRNA stop codon techniques have been used to install photocaged Tyr,[78,99,104,166] Ser,[98] Lys,[84,90,110] Cys,[69,74,97,167] homocysteine (Hcy),[167] and selenocysteine (SeCy) (Figure 15).[165] In addition, the range of model organisms in which this photocaged technology can be deployed has expanded as well, and now includes *E. coli*, *S. cerevisiae*, as well as mammalian cells.[74,84,99]

Surprisingly, relative few alternatives to photocaged UAA incorporation exist for building photocaged proteins. These alternative methods include a single example of total protein synthesis using native chemical ligation (NCL) and, as well as solution-phase photocaging methods, such as Cys *S*-alkylation with a photodegradable active-site ligand.

4.1.2 Total chemical synthesis using SPPS and NCL

The first and only example of total chemical synthesis of photocaged proteins produced a photocaged hen egg lysozyme.[103] Fmoc SPPS was required to synthesize four fragments that were subsequently ligated together to form lysozyme, a 14.3 kDa protein (Figure 16). Lysozyme was synthesized with three photocaged mutants at Lys96, Ser100, and Asp101.

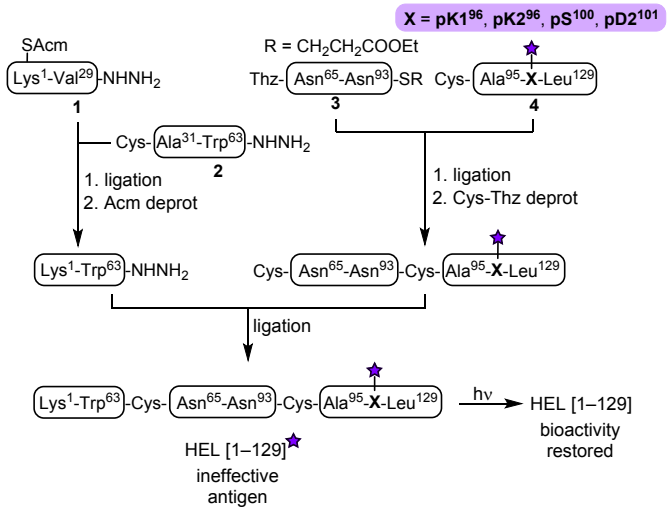

Figure 16. Roadmap for total protein synthesis of a photocaged HEL variants. Four different photocaged amino acids were incorporated within the Ala[95]–Leu[129] and the entire protein subsequently assembled by native chemical ligation.

4.1.3 Solution-phase selective functional group photocaging

Selective photocaging reactions on whole proteins are the third major approach to photocaged proteins. The development of selective protein caging methods has mirrored broader efforts to develop site-selective bioconjugation methods. Solution-phase site-specific photocaging of an active-site side chain is an alternative approach to genetic pAA incorporation. Furthermore, solution-phase methods on whole proteins provide opportunities to develop conceptually different approaches to photocaging, such as PEG conjugation.

Modification of numerous surface-exposed residues with photocleavable polyethylene glycol (PEG) polymers has been pursued as an approach to both inactivate and protect against degradation. A representative example[168] employed Lys modification with a reactive carbonate containing a nitrobenzyl linkage to a large PEG chain (Figure 17a). Numerous PEG chains

attached to the surface had the effect of blocking natural cell lysis activity of the enzyme (PEG-lysozyme, Figure 17a). Upon irradiation, the cell lysis activity is recovered (Figure 17b). The technique produces heterogeneous changes to the protein surface, so reproducibility concerns and other issues regarding heterogeneous bioconjugation products are important caveats. Nonetheless, the method is simple, efficient, and has the distinct advantage of not requiring knowledge about protein structure on an atomic scale.

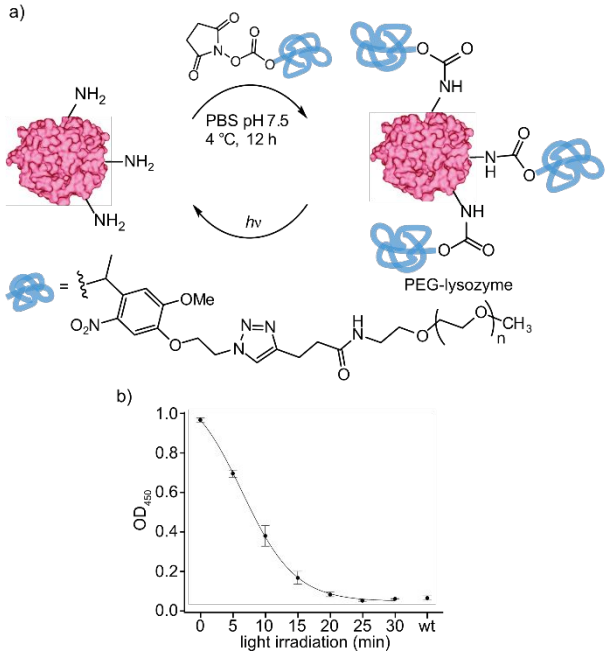

Figure 17. Polymer-conjugate-photocaging of lysozyme using NHS ester under aqueous conditions. (a) Schematic depiction of PEG-photocaging of lysozyme, which places multiple polymer chains at surface Lys residues. (b) OD measurements of *Micrococcus lysodeikticus* consumption by photocaged lysozyme during irradiation time points. Reprinted with permission from *Bioconjugate Chem*. 2010, 21, 8, 1404–1407. Copyright 2010 American Chemical Society.

Achieving site-selective photocaging through reactions on canonical proteins is both a more daunting challenge and important for many applications of photocaging concepts. In rare cases, a unique amino acid residue—typically Cys—may exist in an appropriate location for selective photocaging. Such nucleophilic residues allow the use of reactive electrophiles, such as alkyl bromides or maleimides.[89,169–172] In an extension of these ideas, enzymatic thiophosphorylation can be used to introduce a sulfur-based functional group with singular reactivity.[173] For proteins without surface-exposed Cys, genetic incorporation of a specific Cys residue often represents the most straightforward way to incorporate a uniquely reactive site.

To address the need for photocaging of natural proteins without genetic manipulation, the His-directed catalytic alkenylation of peptide backbone N–H bonds (Figure 9) was also demonstrated on a full-length protein, the soybean trypsin inhibitor (SBTI). Containing a single His residue, reaction of SBTI with boronic acids in the presence of a copper catalyst afforded singly-modified protein products, consistent with a His-directed mechanism. Upon irradiation, disappearance of the desthiobiotin-containing photocage was observed.[86] Photocaging protein backbone structures may be a simple tool to achieve significant alteration to protein structure, although further studies will be needed to establish the efficiency and potential of this approach.

As an alternative to small molecule solution-phase photocaging, site-directed affinity labels take advantage of proximity-driven covalent modification at non-active site amino acids. In an example from Lawrence *et al*.,[169] a peptide-based caging agent was designed to activate fluorescence labelling upon irradiation. Elegantly designed, the caging agent exhibits key moieties that direct the probe near the active site where the probe's maleimide electrophile covalently bonds local Cys 343, effectively labelling the protein. The caging agent also comprises of a fluorescent quencher that is release upon UV irradiation, activating fluorescence.

4.2 Applications of photocaged proteins

This section presents selected examples of the applications of photocaged proteins. We have chosen select examples that convey broad concepts or approaches involving the use of photocaged proteins in living systems, rather than provide a complete catalog of all such examples.

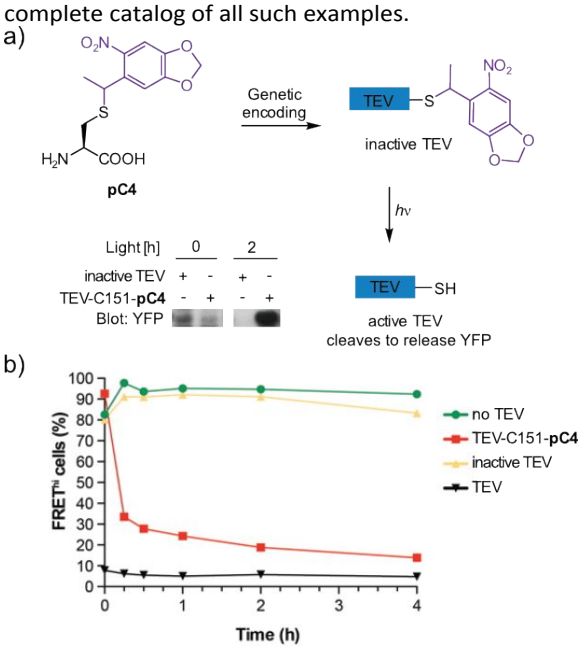

Figure 18. A photocaged TEV protease. (a) Photocaged Cys (**pC4**) was incorporated into mutant TEV protease. Western blot indicating free YFP following the cleavage of CFP-TevS-YFP-V5 by light-activated TEV-C151-**pC4**. (b) FACS analysis of TEV-C151-**pC4** photoactivation in mammalian cells. Percentage of FRET^{hi} over time post-irradiation, confirming TEV protease activation (red). Inactive TEV (yellow) did not show protease activity. Controls: no TEV (green), wild-type TEV (black). Reprinted with permission from *J. Am. Chem. Soc.* 136, 6, 2240. Copyright 2014 American Chemical Society.

4.2.1 Photocaging protein active site: Tobacco Etch Virus (TEV) protease activation

Spatiotemporal variation in enzyme activity provides the basis for protein dynamics in cells and living organisms, and photoactivation of enzyme activity represents one of the most straightforward applications of protein photocaging. Photoactivation of the tobacco etch virus (TEV) protease selectively activates decomposition of proteins containing the

TEV cleavage site (TevS), potentially enabling an optically activated protein knock-out, and the opportunity to probe knock-outs at different cellular developmental stages. Using a photocaged Cys, Chin *et al*. engineered a photocaged TEV protease, TEV-C151-**pC4**, in *E. coli* and mammalian cells.[69] (Figure 18a). To analyze TEV activity in cells, a fusion protein, CFP-TevS-YFP-V5, was engineered containing a cleavage sequence (TevS) between two fluorescent proteins, CFP and YFP. Uncaging TEV-C151-**pC4** with light induced proteolytic cleavage of the TevS sequence, which could be easily visualized by a FRET-based fluorescence activated cell sorting (FRET-FACS, Figure 18b).

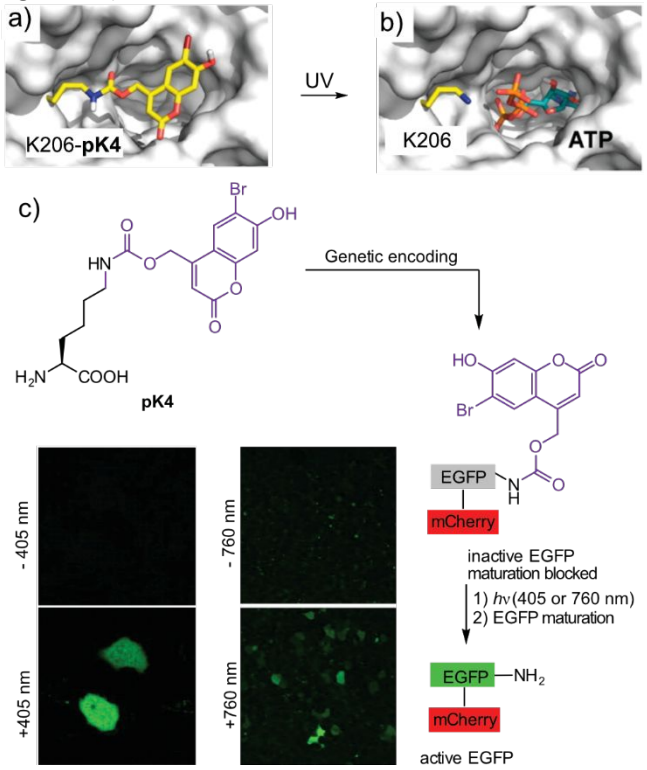

Figure 19. Photoactivated *Photinus pyralis* firefly luciferase (Fluc) using stop codon suppression. (a) Model of Lys206 caged with **pK4**, disrupting a hydrogen bonding network and blocking substrates entering the binding pocket (model based on PDB: 2D1S). (b) Irradiation generates wild-type (active) Fluc structure (PDB: 2D1S). (c) Photocaging of EGFP-mCherry fusion protein with **pK4**. Fluorescence is recovered following uncaging and folding of EGFP. (inset) Confocal microscopy of cells before and after irradiation with 405- or 760-nm light. Reprinted with permission from *J. Am. Chem. Soc.* 136, 44, 15551. Copyright 2014 American Chemical Society.

4.2.2 Photocaging protein active sites: Photoactivation of luciferase and GFP luminescence

Photocaging key residues is a conceptually straightforward way to disrupt function. In studies from the Deiters lab, this approach was implemented in two model proteins: photocaging the active site luciferase enzymes (Figure 19a-b) and photocaging GFP fluorescence (Figure 19c).[90,167] The authors began studies by photocaging *Renilla reniformis* luciferase (*Renilla*) and *Photinus pyralis* firefly luciferase (Fluc) at key residues. According to modelling studies, Fluc has a key Lys (K206)[90] at the entry channel of the active site for the substrates luciferin and ATP. When K206 was photocaged as **pK4**, luciferin and ATP are blocked from entering the active site, thus deactivating the protein (Figure 19a). *Renilla* demonstrated similar activity with C124[167] was photocaged with **pC7**. Enzymatic activity was restored following UV irradiation in both the *Renilla* and Fluc examples. In the case of coumarin-photocaged Fluc, one- and two-photon uncaging was demonstrated.[90] Uncaged Fluc is generated by irradiation with 365-nm light, and a 30-fold enhancement of chemiluminescence indicated recovery of the enzymatic activity.

This photocaging technique was also used to produce a light triggered EGFP. EGFP-mCherry fusion protein was photocaged with **pK4**. Lys photocaging disrupted the folding of EGFP and demonstrated the sensitivity of these folding motifs to perturbation (Figure 19c). Following irradiation with 405- or 760-nm light, EGFP folds and becomes fluorescent (inset, Figure 19c). These examples of photocaging fluorescent and bioluminescent proteins demonstrate the use of optical control of protein active sites as tools for probing cellular pathways.

4.2.3 Applications of solution-phase protein photocaging

Using chemical posttranslational modification to install a photocaged residue is limited to a few unique cases. The scarcity and unique reactivity of Cys means that Cys alkylation can be used for such purposes. Cofilin is a protein which regulates assembly/disassembly of F-actin through phosphorylation of Ser3.[174] Cofilin was photocaged through production of a Ser3Cys mutant, followed by solution-phase alkylative photocaging with 2-nitrobenzylbromide alkylating reagent at this key position.[170] Mutant Ser3Cys remained active prior to photocaging, but was inactive after alkylation. (bottom, Figure 20). Upon irradiation, the uncaged cofilin activity was restored as indicated by cleavage sites observed in the F-actin filament (top, Figure 20).

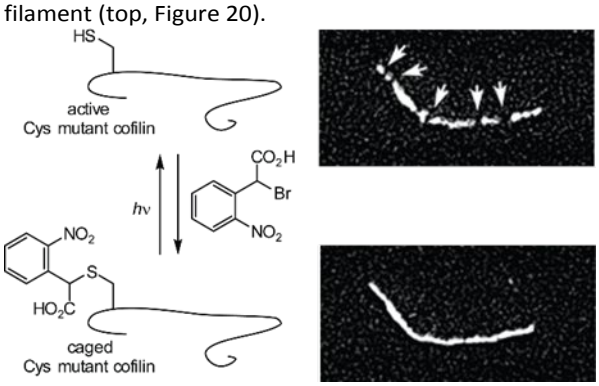

Figure 20. Site-selective photocaging of cofilin, an actin regulatory protein that severs actin filaments. A unique engineered Cys residue allowed selective cofilin caging. (top image) Light microscope image of F-actin in presence of uncaged cofilin with cleavage sites (white arrows). (bottom image) Light microscope image of intact F-actin in presence of caged cofilin. Reprinted with permission from *J. Am. Chem. Soc.* 124, 11, 2440. Copyright 2002 American Chemical Society.

Similar Cys reactivity has been used to build photocaged ion channel proteins by chemical posttranslational modification, in an approach that complements the UAA-based method described above.[89] In this example, a transmembrane ion channel porin (OmpG) was genetically encoded to contain two Cys residues within the transmembrane pore.[89] OmpG is a 14-stranded β-barrel structure consisting of a single amino acid

chain. Simple *S*-alkylation with a photolabile 7-(diethylamino)-4-(hydroxymethyl)-coumarin bromide (DEACM) at the engineered Cys residues serves as a physical blockage of the ion channel (Figure 21). Of note, the authors observed that alkylative photocaging can take place in either the native state, or in a denatured state prior to refolding. The authors demonstrated 54% increase in ion conduction following uncaging of the physical blockage.

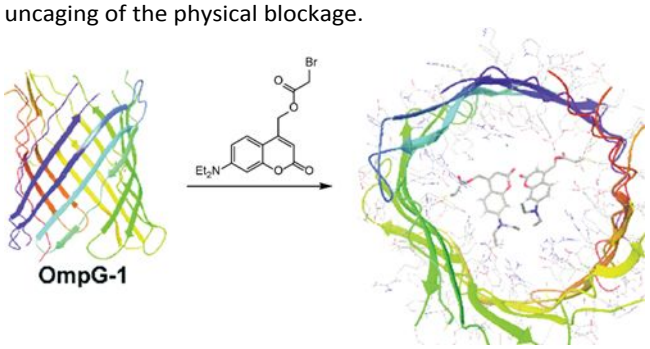

Figure 21. Synthesis of photocaged OmpG-2 with DEACM photocaging group to produce the photocaged transmembrane porin. Unique Cys residues engineered within the pore opening allowed selective caging of the protein Cys (PDB: 4CTD). Reproduced from Ref. 89 with permission from the Royal Society of Chemistry.

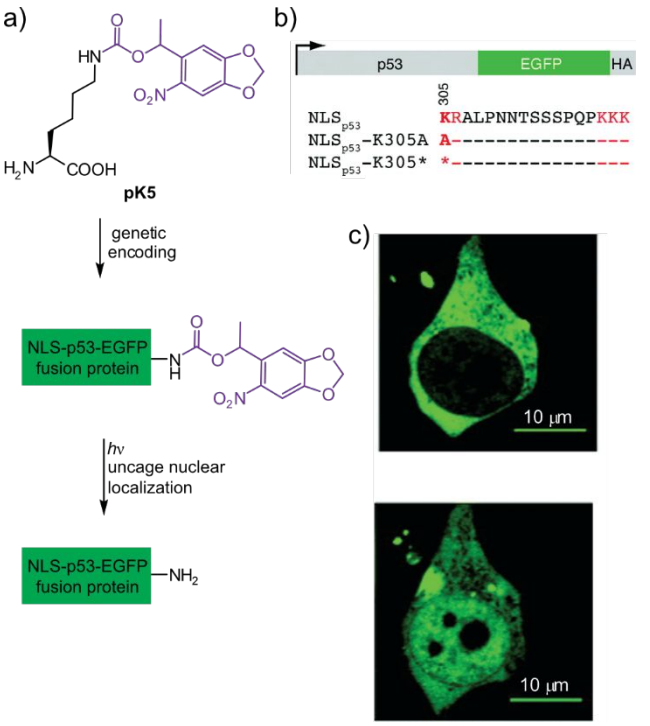

Figure 22. Photocaged Lys for controlling protein localization within cells. (a) Schematic representation of **pK5** incorporation into NLS-p53-EGFP fusion protein and subsequence uncaging. (b) Sequence design of NLS-p53 fusion proteins. (c) Confocal microscopy indicating cellular localization of the p53-EGFP fusions before and 50 min after photolysis (5 s, 365 nm, 1.2 mW/cm2). Reprinted with permission from *J. Am. Chem. Soc.* 132, 12, 4086. Copyright 2010 American Chemical Society.

4.2.4 Probing protein localization within mammalian cells

The vast complexity of living systems derives in large part from epigenetic factors. Engineering desired biological outcomes requires temporal and subcellular spatial control over protein expression and function. Understanding natural function, similarly, depends on controlling and understanding time-resolved changes in protein activity. Photocaging techniques are uniquely qualified for these challenges, in part due to the small steric size of photocaging groups and the development of methods for expressing proteins incorporating an unnatural pAA. The caged Lys **pK5** is among the most common pAA for genetic incorporation with. Incorporating **pK5** in the nuclear localization sequences (NLS) of a p53–EGFP fusion protein (Figure 22a)[84] resulted in incorrect localization of the fusion protein within the cytosol of HEK293 cells. After irradiation with light, the p53–EGFP fusion exhibited large changes in subcellular localization, with significant amounts of the p53–EGFP fusion found in the nucleus (Figure 22c).

4.2.5 A photocaged tyrosine for controlled STAT1 phosphorylation

Phosphorylation/dephosphorylation cascades are a key mediator of signal transduction processes. Incorrectly regulated phosphorylation pathways are a hallmark of many disease states,[175–177] and external control of phosphorylation state is important to our understanding of these key disease pathways, in addition to representing a potentially important avenue to engineer new biological function. STAT1, a transcription promoter, undergoes phosphorylation-induced dimerization and translocation to the nucleus, where the protein binds DNA and induces an immune response (Figure 23).[104] When a site-specific photocaged Tyr was genetically encoded into STAT1, phosphorylation is prevented and, thus, downstream signalling (Figure 23).[104] Western blot analysis was then used to assess subsequent phosphorylation after photo-induced uncaging to reveal the natural Tyr residue (Figure 23, blot).[178]

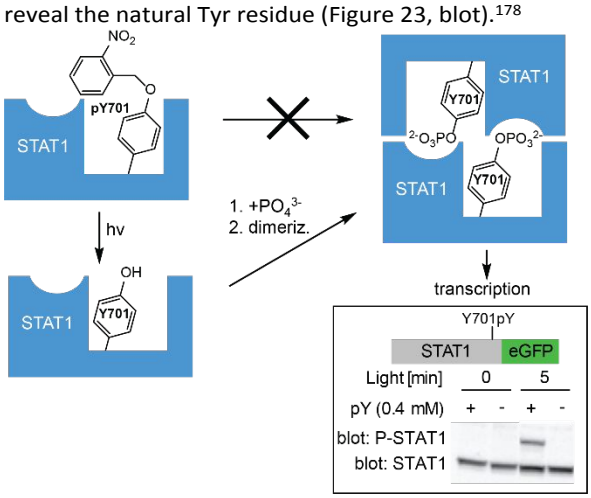

Figure 23. Photocontrol of STAT1 phosphorylation. A cartoon model of the interferon JAK/STAT1 phosphorylation pathway that can blocked by photocaging Tyr701. Western blot of pTyr-STAT1-GFP fusion protein where phosphorylation of STAT1-GFP increases over time with UV irradiation (saturating at 5 min, blot: P-STAT1). STAT1 blot reprinted with permission from *J. Am. Chem. Soc.* 134, 29, 11912. Copyright 2012 American Chemical Society.

4.2.6 Photocaged T7-RNA polymerase for controlled gene expression

Gene and protein expression are controlled at both the transcriptional and translational levels, giving the cell a plethora of potential control points. Protein deactivation can have profound and sometimes disastrous consequences for cells, and

site-specific protein photocaging has proven a useful tool to probe these effects.[166] In one important study, photocaging was used to probe deactivation of mitosis genes. To examine the impacts of gene deactivation, a T-7 RNA polymerase was encoded with photocaged Lys (**pK5**) in mammalian cells, through standard UAA incorporation methods. As a proof of concept, a T-7 RNA polymerase with a photocaged Try residue (**pY**) was designed and produced in *E. coli* through standard UAA incorporation methods. This photocaging blocked GFP expression.[166] In a follow up to this methodology for controlling gene expression, T7-RNA polymerase was photocaged at Lys (**pK5**) in mammalian cells. This study showed a light-triggered expression of luciferase, GFP, and short hairpin RNA (shRNA).[110] Using the photocontrolled shRNA expression, light-triggered inhibition of Eg5 gene, which encodes a motor protein required for mitosis[179] was developed to study interfering RNA pathways in gene silencing. The photocaged T7-RNA inhibited expression of shRNA; thus, cells divided naturally (Figure 24, left). Photoactivation of T7-RNA promotes the synthesis of shRNA, inhibiting the Eg5 gene and resulted in binucleated cells during mitosis (Figure 24, right).

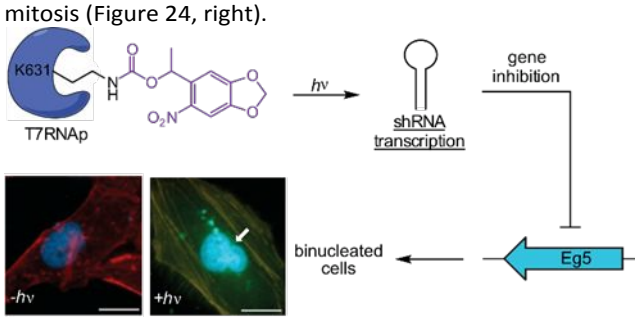

Figure 24. RNA interference triggers a binucleated cell phenotype (white arrow) through light-triggered shRNA inhibition of Eg5 using the caged T7RNAp. Scale bars = 20 µm. Cell images reprinted with permission from *J. Am. Chem. Soc.* 135, 36, 13433. Copyright 2013 American Chemical Society.

4.2.7 Photocaged ion channels

Potassium channels are membrane proteins that play crucial roles in regulating neuronal excitability, action potential cessation, hormone secretion, heart rate, and salt balance.[180] A photocaged Cys (**pC5**) residue was employed within a photocaged inwardly-rectifying potassium channel (Kir2.2) in embryonic mouse neocortex cells (Figure 25) and rat hippocampal neurons.[97] Cys 169 was identified as a key residue, allowing ion flow into the channel. When Kir2.2 is photocaged with **pC5**, ion flow is blocked. To incorporate **pC5**, the amino acid was introduced as a dipeptide **pC5**-Ala to enhance transport into cells. Dipeptide pC4-Ala is readily hydrolyzed by cytosolic peptidases to the free **pC5** for incorporation into Kir2.2 via standard UAA incorporation methods. Ion channel current in embryonic mouse neurons was measured upon photoactivation of Kir2.2 in neocortical acute slices (Figure 25b). Following UV irradiation, the current changed dramatically at potentials below a turn-on potential of –60 mV. The current measured at –90 mV rose from −17 pA (black) to −317 pA (blue). Among control experiments, it was determined that Ba^{2+} inhibits the conduction of the photo-induced channels in a manner similar to native channels (orange).

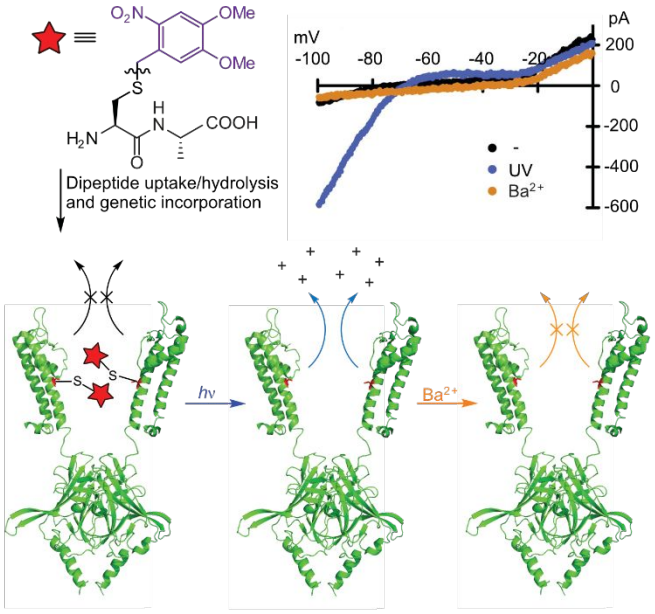

Figure 25. Incorporation of **pC5** into potassium channel Kir2.2 at C169 stops ion current. (top, right) Mouse neocortical neurons (I-V) plot. When irradiated, C169 is uncaged, allowing the flow of positive ions through the channel below ca. –70 mV for Kir2.2-expressing neurons (blue). When inhibited with Ba^{2+}, ion current is stopped (orange). I-V plot reprinted from reference 97 with permission from Elsevier.

4.2.8 Photocaging of fast inteins for controlled protein splicing

Light-promoted protein activation has most commonly been achieved by modifying residues on mature proteins. Disrupting intein splicing and thus preventing the maturation of translated sequences can be viewed as a complementary strategy. The approach takes advantage of the predictable mechanistic role of Cys residues in intein splicing reactivity. In a study by Ai *et al*., a photocaged Cys residue (**pC5**) was incorporated into the N-terminal region of the intein coding region of mCherry and separately into the catalytic domain of the human Tyr kinase, Src, using the Nostoc punctiforme (Npu) DnaE intein.[70] As one of the most well-characterized and efficient inteins, Npu is compatible with a variety of flanking extein sequences and has a splicing half-life of ~60 s at 37 °C.[181,182] As a proof of concept, cells incorporating the photocaged mCherry intein construct did not exhibit mCherry fluorescence until after UV irradiation, indicating the dependence of mCherry maturation on **pC5** uncaging.. In the Src example, *Npu* intein was incorporated within the Src protein sequence, creating a “photo-spliceable” kinase analogue (Figure 26a) expressed in HEK cells.[70] For efficient splicing, the photocaged Src proteins also contained the S342C mutation to install the Cys necessary for enhanced splicing efficiency.[182] Using a KRas-Src sensor (ECFP/YPet FRET reporter) for Src activity,[183] the photoactivation of intein excision and maturation of Src was analyzed. HEK 293K cells expressing the KRas-Src sensor and photocaged Src proteins were treated with UV irradiation and fluorescence quantification was measure on the lysed cells. FRET-based imaging demonstrated dramatically higher response of the KRas-Src sensor after UV irradiation (Figure 26b). Light-based control of intein splicing is an efficient method for controlled

protein function with a fast response in cells,[184] and related approaches have begun to appear.[185]

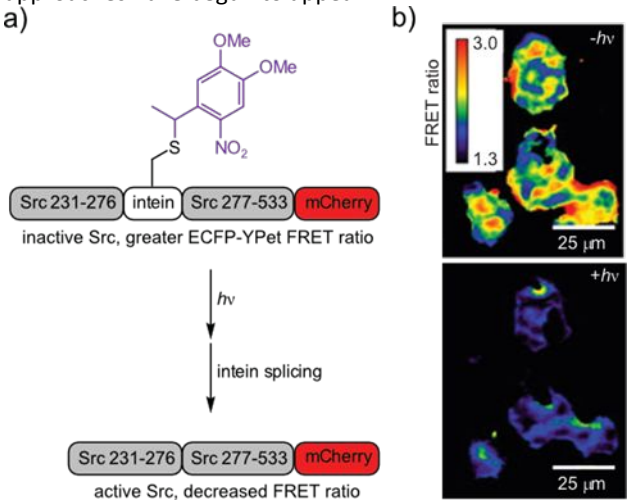

Figure 26. A light-triggered intein splicing activates of Src. (a) Schematic representation of Src-mCherry fusion protein before and after photoactivation of intein excision. (b) Post-treatment images of pseudocolored fluorescence ratio (YPet/ECFP) images of F1 expressing HEK 293T cells treated with UV irradiation indicating the activation of Src based on decreased FRET ratio. Color bar: fluorescence ratio (YPet/ECFP). Adapted with permission from *J. Am. Chem. Soc.* 137, 6, 2155. Copyright 2015 American Chemical Society.

4.2.9 Manipulation of protein interactions using photocaged proteins

A remarkable and noteworthy protein synthesis effort served as the basis for a photocaging approach to study protein-protein interactions in live cells. Total chemical synthesis of hen egg lysozyme (HEL) was used, as an alternative to genetic UAA incorporation, in hopes that systematic probing of a variety of photocaging locations might shed fundamental light on differences in photocaging efficiency.[103] By caging multiple residues through total synthesis, the optimal location and photocage were identified for HEL and activity upon irradiation was assessed. HEL, a model antigen, is recognized by B-cells through a membrane bound HEL-specific antibody (HyHEL-10) on the cell surface.[186] Residues Lys96, Ser100, and Asp101 were screened for activity in binding the HyHEL-10 receptor, and Lys96 was identified as a key residue for binding HyHEL-10 using ELISA assays. It was also determined that photocaging Lys96 with 1-(2-nitrophenyl)ethyl (**pK1**) successfully inhibited the protein-protein interaction and, importantly, restored antigenicity after uncaging (Figure 27). With an optimized photocaged antigen in hand, the uncaging and subsequent B cell receptor (BCR) interactions were measured using total internal reflection fluorescence microscopy (TIRF, Figure 27, left). Alexa Fluor 647-labeled MD4 primary B cells were exposed to a glass slide containing immobilized, photocaged HEL-**pK1**. Irradiation activated B cell spreading responses to form microclusters and accumulation of BCRs into the B cells immunological synapse. The ratio of the mean fluorescence intensity (mFI) for the accumulation of BCRs was measured over time after UV irradiation and indicated a 5-fold increase in the mean fluorescence ratio following irradiation. This indicates the uncaging of HEL-**pK1** and subsequent protein-protein interactions between HEL and HyHEL-10 on the cell surface.

Next, oscillation of Ca^{2+} levels were measured in response to the antigen-antibody interaction of HEL and HyHel-10 (Figure 27, right).[103] Calcium imaging was performed by prestaining the B-cells with calcium probe Fluo-4 and placing the cells on cover slides. HEL-**pK1** was flowed over the cells. Only basal amounts of calcium were detected before UV irradiation, and no oscillation was observed. Following irradiation, uncaged HEL-**pK1** was able to interact with the B-cells, inducing an influx of calcium and successive oscillation at a cycle of 85-90 s. These data indicate light-dependent activation of HEL-HyHEL-10 protein-protein interactions.

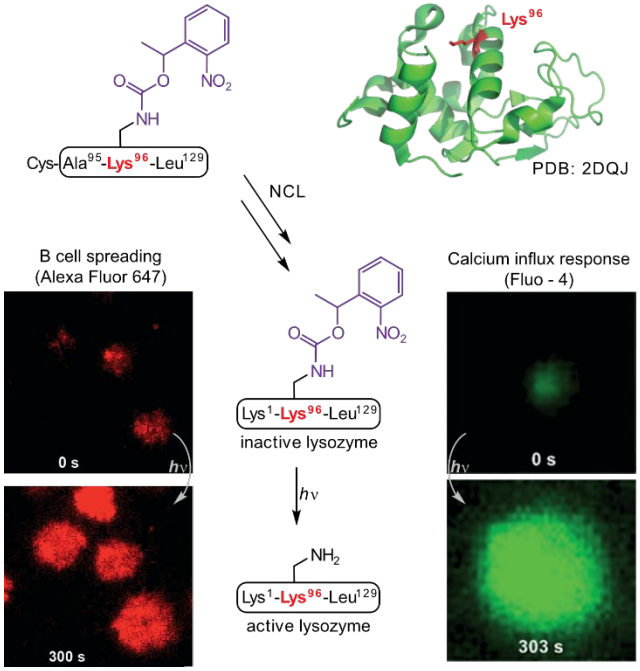

Figure 27. Total protein synthesis of a photocaged hen egg lysozyme (HEL-**pK1**^{96}, PDB: 2DQJ) by native chemical ligation incorporating a photocaged Ala95–Leu129 peptide. (left) Fluorescence images of UV irradiation of HEL-**pK1**^{96} caused B cell spreading responses and accumulation of BCRs into the B cells immunological synapse. (right) Fluorescence images of UV irradiation of HEL-**pK1**^{96}-induced calcium influx and oscillation as indicated by increased in green fluorescence. Adapted from Ref. 103 with permission from the Royal Society of Chemistry.

5. Conclusions

Light can be a uniquely non-invasive approach to triggered folding, maturation, and activity of peptides and proteins. Spatial and temporal controls of protein activity with light are important features of photocaged approaches that are difficult to achieve with chemical reagents. These attributes have allowed synthetic triumphs that became possible only in the past decade: the first photocaged protein *in vivo*, first total synthesis of a photocaged protein, first solution-phase backbone modification, and a plethora of creative advances in NCL, to name a few.

However, there are several chemical themes that stand out as important future directions: (1) Photocaging has mostly targeted heteroatom-containing sidechains. Furthermore,

predicting sites of effective photocaging can be difficult, such that the union of effective photocaging sites and readily accessed photocages may be limited. In one example, Liu *et al.* reported photocaging a specific lysine was necessary to effectively deplete HEL-HyHEL-10 recognition in their study of photocaged HEL,[103] while other reasonable photocaging targets failed. (2) Chemically photocaging full-length, natural sequences remains a challenge, with selective alkylation of an engineered cysteine side chain offering probably the most predictably effective approach.[89] (3) Photocaging at red-shifted wavelengths in the visible or near-IR has clear advantages due to tissue penetration concerns and/or UV-induced DNA damage. The development of visible light-sensitive photocages and two-photon photocages has been an important development that will likely continue.[66,67,87,95] (4) Predicting effective photocaged target structures requires effective interplay of computational and experimental approaches, and computational advances should improve some of the empirical nature of this process. (5) Protein complexity is a challenge, and the contrast between techniques available for peptide versus protein substrates is extensive, paralleling the broader bioconjugation field. (6) Analytical capabilities and investigations remain a key area of need. In vivo and in cellulo dosing requires an understanding of uncaging efficiencies and kinetics, which are often to measure in vivo, as opposed to under controlled conditions in a test tube. Alternative fates of photo-excited intermediates and especially byproducts represent another crucial piece of understanding that is insufficiently well understood for many systems.

The successes, including those outlined here, are beginning to demonstrate some broadly effective and predictable photocaging approaches, practical implementations that allow these tools to be used in the hands of diverse researchers to address diverse problems. The field seems poised to move more broadly beyond chemical experts demonstrating proof of concept experiments, and into a more broadly used tool. Certainly, this development will occur in tandem with the development of fundamental advances in new methods, new caging approaches, and new reagents.

Author Contributions

A.E.M and Z.T.B. jointly conceived, researched, wrote, and edited this contribution.

Conflicts of interest

There are no conflicts to declare.

Acknowledgements

We acknowledge support from the Robert A. Welch Foundation Research Grant C-1680 and the National Science Foundation (CHE-1055569 and CHE-1904865).

Notes and references

1 K. Hüll, J. Morstein and D. Trauner, *Chem. Rev.*, 2018, **118**, 10710–10747.
2 W. A. Velema, W. Szymanski and B. L. Feringa, *J. Am. Chem. Soc.*, 2014, **136**, 2178–2191.
3 G. H. Patterson, *Curr. Protoc. Cytom.*, 2011, **57**, 12.23.1-12.23.12.
4 S. Wong, A. A. Mosabbir and K. Truong, *PLOS ONE*, 2015, **10**, e0135965.
5 A. M. Weber, J. Kaiser, T. Ziegler, S. Pilsl, C. Renzl, L. Sixt, G. Pietruschka, S. Moniot, A. Kakoti, M. Juraschitz, S. Schrottke, L. L. Bryant, C. Steegborn, R. Bittl, G. Mayer and A. Möglich, *Nat Chem Biol*, 2019, **15**, 1085–1092.
6 G. Zheng, L. Cochella, J. Liu, O. Hobert and W. Li, *ACS Chem. Biol.*, 2011, **6**, 1332–1338.
7 Y. Shigeri, Y. Tatsu and N. Yumoto, *Pharmacol. Ther.*, 2001, **91**, 85–92.
8 D. S. Lawrence, *Curr. Opin. Chem. Biol.*, 2005, **9**, 570–575.
9 W. H. So, C. T. T. Wong and J. Xia, *Chin. Chem. Lett.*, 2018, **29**, 1058–1062.
10 C. W. Riggsbee and A. Deiters, *Trends Biotechnol.*, 2010, **28**, 468–475.
11 S. R. Adams and R. Y. Tsien, *Annu. Rev. Physiol.*, 1993, **55**, 755–784.
12 M. Bose, D. Groff, J. Xie, E. Brustad and P. G. Schultz, *J. Am. Chem. Soc.*, 2006, **128**, 388–389.
13 U. Kusebauch, S. A. Cadamuro, H. Musiol, M. O. Lenz, J. Wachtveitl, L. Moroder and C. Renner, *Angew. Chem., Int. Ed.*, 2006, **45**, 7015–7018.
14 G. A. Woolley, A. S. I. Jaikaran, M. Berezovski, J. P. Calarco, S. N. Krylov, O. S. Smart and J. R. Kumita, *Biochemistry*, 2006, **45**, 6075–6084.
15 P. Gorostiza, M. Volgraf, R. Numano, S. Szobota, D. Trauner and E. Y. Isacoff, *Proc. Natl. Acad. Sci. U.S.A.*, 2007, **104**, 10865–10870.
16 Y. Zhang, F. Erdmann and G. Fischer, *Nat. Chem. Biol.*, 2009, **5**, 724–726.
17 J. Broichhagen and D. Trauner, *Curr. Opin. Chem. Biol.*, 2014, **21**, 121–127.
18 J. A. Frank, M. Moroni, R. Moshourab, M. Sumser, G. R. Lewin and D. Trauner, *Nat. Commun.*, 2015, **6**, 7118.
19 C. K. McKenzie, I. Sanchez-Romero and H. Janovjak, in *Novel Chemical Tools to Study Ion Channel Biology*, eds. C. Ahern and S. Pless, Springer New York, New York, NY, 2015, pp. 101–117.
20 R. Mart and R. Allemann, *Chem. Commun.*, 2016, **52**, 12262–12277.
21 D. B. Konrad, J. A. Frank and D. Trauner, *Chem. - Eur. J.*, 2016, **22**, 4364–4368.
22 H. Sun, L. Zhao, T. Wang, G. An, S. Fu, X. Li, X. Deng and J. Liu, *Chem. Commun.*, 2016, **52**, 6001–6004.
23 J. Kuil, L. T. M. van Wandelen, N. J. de Mol and R. M. J. Liskamp, *J. Pept. Sci.*, **15**, 685–691.
24 P. Klán, T. Šolomek, C. G. Bochet, A. Blanc, R. Givens, M. Rubina, V. Popik, A. Kostikov and J. Wirz, *Chem. Rev.*, 2013, **113**, 119–191.
25 V. N. R. Pillai, *Synthesis*, 1980, **1980**, 1–26.
26 J. H. Kaplan, B. Forbush and J. F. Hoffman, *Biochemistry*, 1978, **17**, 1929–1935.
27 G. Zhou, F. Khan, Q. Dai, J. E. Sylvester and S. J. Kron, *Mol. BioSyst.*, 2012, **8**, 2395–2404.
28 X. M. M. Weyel, M. A. H. Fichte and A. Heckel, *ACS Chem. Biol.*, 2017, **12**, 2183–2190.
29 A. R. Chandrasekaran, J. A. Punnoose, V. Valsangkar, J. Sheng and K. Halvorsen, *Chem. Commun.*, 2019, **55**, 6587–6590.

30 Z. Vaníková, M. Janoušková, M. Kambová, L. Krásný and M. Hocek, *Chem Sci*, 2019, **10**, 3937–3942.
31 S. G. Chaulk and A. M. MacMillan, *Nat. Protoc.*, 2007, **2**, 1052–1058.
32 J. M. Govan, D. D. Young, H. Lusic, Q. Liu, M. O. Lively and A. Deiters, *Nucleic Acids Res*, 2013, **41**, 10518–10528.
33 W. A. Velema, A. M. Kietrys and E. T. Kool, *J. Am. Chem. Soc.*, 2018, **140**, 3491–3495.
34 D. Zhang, C. Y. Zhou, K. N. Busby, S. C. Alexander and N. K. Devaraj, *Angew Chem Int Ed Engl*, 2018, **57**, 2822–2826.
35 E. V. Moroz-Omori, D. Satyapertiwi, M.-C. Ramel, H. Høgset, I. K. Sunyovszki, Z. Liu, J. P. Wojciechowski, Y. Zhang, C. L. Grigsby, L. Brito, L. Bugeon, M. J. Dallman and M. M. Stevens, *ACS Cent. Sci.*, 2020, **6**, 695–703.
36 W. Zhou, W. Brown, A. Bardhan, M. Delaney, A. S. Ilk, R. R. Rauen, S. I. Kahn, M. Tsang and A. Deiters, *Angew. Chem. Int. Ed.*, 2020, **59**, 8998–9003.
37 S. Berlin, S. Szobota, A. Reiner, E. C. Carroll, M. A. Kienzler, A. Guyon, T. Xiao, D. Trauner and E. Y. Isacoff, *eLife*, 2016, **5**, e12040.
38 P. P. Goswami, A. Syed, C. L. Beck, T. R. Albright, K. M. Mahoney, R. Unash, E. A. Smith and A. H. Winter, *J. Am. Chem. Soc.*, 2015, **137**, 3783–3786.
39 Y. Venkatesh, Y. Rajesh, S. Karthik, A. C. Chetan, M. Mandal, A. Jana and N. D. P. Singh, *J. Org. Chem.*, 2016, **81**, 11168–11175.
40 A. Li, C. Turro and J. J. Kodanko, *Chem. Commun.*, 2018, **54**, 1280–1290.
41 J. Olejnik, S. Sonar, E. Krzymañska-Olejnik and K. J. Rothschild, *Proc. Natl. Acad. Sci. U.S.A.*, 1995, **92**, 7590–7594.
42 J. Olejnik, E. Krzymanska-Olejnik and K. J. Rothschild, *Nucleic Acids Res.*, 1998, **26**, 3572–3576.
43 S. V. Wegner, O. I. Sentürk and J. P. Spatz, *Sci. Rep.*, 2015, **5**, 18309.
44 K. K. Behara, Y. Rajesh, Y. Venkatesh, B. R. Pinninti, M. Mandal and N. D. P. Singh, *Chem. Commun.*, 2017, **53**, 9470–9473.
45 J. A. Peterson, C. Wijesooriya, E. J. Gehrmann, K. M. Mahoney, P. P. Goswami, T. R. Albright, A. Syed, A. S. Dutton, E. A. Smith and A. H. Winter, *J. Am. Chem. Soc.*, 2018, **140**, 7343–7346.
46 T. Sõrmus, D. Lavogina, E. Enkvist, A. Uri and K. Viht, *Chem. Commun.*, 2019, **55**, 11147–11150.
47 C. de Gracia Lux, J. Lux, G. Collet, S. He, M. Chan, J. Olejniczak, A. Foucault-Collet and A. Almutairi, *Biomacromolecules*, 2015, **16**, 3286–3296.
48 L. A. Haines, K. Rajagopal, B. Ozbas, D. A. Salick, D. J. Pochan and J. P. Schneider, *J. Am. Chem. Soc.*, 2005, **127**, 17025–17029.
49 R. Y. Tam, L. J. Smith and M. S. Shoichet, *Acc. Chem. Res.*, 2017, **50**, 703–713.
50 B. Amit, D. A. Ben-Efraim and A. Patchornik, *J. Am. Chem. Soc.*, 1976, **98**, 843–844.
51 A. D. Cohen, C. Helgen, C. G. Bochet and J. P. Toscano, *Org. Lett.*, 2005, **7**, 2845–2848.
52 A. Hassner, D. Yagudayev, T. K. Pradhan, A. Nudelman and B. Amit, *Synlett*, 2007, **2007**, 2405–2409.
53 H. Boudebous, B. Košmrlj, B. Šket and J. Wirz, *J. Phys. Chem. A*, 2007, **111**, 2811–2813.
54 X. Dai, Y. Yu, K. Liu and H. Su, *Chin. J. Chem. Phys.*, 2016, **29**, 91–98.
55 C. Ma, W. M. Kwok, H.-Y. An, X. Guan, M. Y. Fu, P. H. Toy and D. L. Phillips, *Chemistry – A European Journal*, 2010, **16**, 5102–5118.
56 A. Schönberg, A. K. Fateen and S. M. A. R. Omran, *J. Am. Chem. Soc.*, 1956, **78**, 1224–1225.
57 A. Chaudhuri, Y. Venkatesh, K. K. Behara and N. D. P. Singh, *Org. Lett.*, 2017, **19**, 1598–1601.
58 V. X. Truong, F. Li and J. S. Forsythe, *Biomacromolecules*, 2018, **19**, 4277–4285.
59 L. Fournier, I. Aujard, T. Le Saux, S. Maurin, S. Beaupierre, J.-B. Baudin and L. Jullien, *Chem. - Eur. J.*, 2013, **19**, 17494–17507.
60 T. Furuta, S. S.-H. Wang, J. L. Dantzker, T. M. Dore, W. J. Bybee, E. M. Callaway, W. Denk and R. Y. Tsien, *Proc. Natl. Acad. Sci. U.S.A.*, 1999, **96**, 1193–1200.
61 C. A. Hammer, K. Falahati, A. Jakob, R. Klimek, I. Burghardt, A. Heckel and J. Wachtveitl, *J. Phys. Chem. Lett.*, 2018, **9**, 1448–1453.
62 Q. Lin, L. Yang, Z. Wang, Y. Hua, D. Zhang, B. Bao, C. Bao, X. Gong and L. Zhu, *Angew. Chem. Int. Ed. Engl.*, 2018, **57**, 3722–3726.
63 R. Schmidt, D. Geissler, V. Hagen and J. Bendig, *J. Phys. Chem. A*, 2007, **111**, 5768–5774.
64 V. R. Shembekar, Y. Chen, B. K. Carpenter and G. P. Hess, *Biochemistry*, 2007, **46**, 5479–5484.
65 M. Bojtár, A. Kormos, K. Kis-Petik, M. Kellermayer and P. Kele, *Org. Lett.*, 2019, **21**, 9410–9414.
66 Y. Becker, E. Unger, M. A. H. Fichte, D. A. Gacek, A. Dreuw, J. Wachtveitl, P. J. Walla and A. Heckel, *Chem. Sci.*, 2018, **9**, 2797–2802.
67 M. M. Mahmoodi, D. Abate-Pella, T. J. Pundsack, C. C. Palsuledesai, P. C. Goff, D. A. Blank and M. D. Distefano, *J. Am. Chem. Soc.*, 2016, **138**, 5848–5859.
68 J. A. Barltrop, P. J. Plant and P. Schofield, *Chem. Commun. (London)*, 1966, **0**, 822–823.
69 D. P. Nguyen, M. Mahesh, S. J. Elsässer, S. M. Hancock, C. Uttamapinant and J. W. Chin, *J. Am. Chem. Soc.*, 2014, **136**, 2240–2243.
70 W. Ren, A. Ji and H. Ai, *J. Am. Chem. Soc.*, 2015, **137**, 2155–2158.
71 A. B. Smith, S. N. Savinov, U. V. Manjappara and I. M. Chaiken, *Org. Lett.*, 2002, **4**, 4041–4044.
72 K. Curley and D. S. Lawrence, *J. Am. Chem. Soc.*, 1998, **120**, 8573–8574.
73 H.-M. Lee, M. A. Priestman and D. S. Lawrence, *J. Am. Chem. Soc.*, 2010, **132**, 1446–1447.
74 N. Wu, A. Deiters, T. A. Cropp, D. King and P. G. Schultz, *J. Am. Chem. Soc.*, 2004, **126**, 14306–14307.
75 J. Pan and K. S. Carroll, *Org. Lett.*, 2015, **17**, 6014–6017.
76 W. F. Veldhuyzen, Q. Nguyen, G. McMaster and D. S. Lawrence, *J. Am. Chem. Soc.*, 2003, **125**, 13358–13359.
77 J. C. Miller, S. K. Silverman, P. M. England, D. A. Dougherty and H. A. Lester, *Neuron*, 1998, **20**, 619–624.
78 S. E. Cellitti, D. H. Jones, L. Lagpacan, X. Hao, Q. Zhang, H. Hu, S. M. Brittain, A. Brinker, J. Caldwell, B. Bursulaya, G. Spraggon, A. Brock, Y. Ryu, T. Uno, P. G. Schultz and B. H. Geierstanger, *J. Am. Chem. Soc.*, 2008, **130**, 9268–9281.
79 X. Xie, Y. Yang, Y. Yang, H. Zhang, Y. Li and X. Mei, *Drug Deliv.*, 2016, **23**, 2445–2456.
80 Y. Ohmuro-Matsuyama and Y. Tatsu, *Angew. Chem. Int. Ed.*, 2008, **47**, 7527–7529.
81 J. P. Olson, H.-B. Kwon, K. T. Takasaki, C. Q. Chiu, M. J. Higley, B. L. Sabatini and G. C. R. Ellis-Davies, *J. Am. Chem. Soc.*, 2013, **135**, 5954–5957.
82 D. Ramesh, R. Wieboldt, A. P. Billington, B. K. Carpenter and G. P. Hess, *J. Org. Chem.*, 1993, **58**, 4599–4605.
83 L. Awad, N. Jejelava, R. Burai and H. A. Lashuel, *ChemBioChem*, 2016, **17**, 2353–2360.
84 A. Gautier, D. P. Nguyen, H. Lusic, W. An, A. Deiters and J. W. Chin, *J. Am. Chem. Soc.*, 2010, **132**, 4086–4088.
85 O. S. Walker, S. J. Elsässer, M. Mahesh, M. Bachman, S. Balasubramanian and J. W. Chin, *J. Am. Chem. Soc.*, 2016, **138**, 718–721.

86 A. E. Mangubat-Medina, S. C. Martin, K. Hanaya and Z. T. Ball, *J. Am. Chem. Soc.*, 2018, **140**, 8401–8404.
87 A. E. Mangubat-Medina, H. O. Trial, R. D. Vargas, M. T. Setegne, T. Bader, M. D. Distefano and Z. T. Ball, *Org. Biomol. Chem.*, 2020, **18**, 5110–5114.
88 P. J. Salveson, S. Haerianardakani, A. Thuy-Boun, A. G. Kreutzer and J. S. Nowick, *J. Am. Chem. Soc.*, 2018, **140**, 5842–5852.
89 J. Kahlstatt, P. Reiß, T. Halbritter, L.-O. Essen, U. Koert and A. Heckel, *Chem. Commun.*, 2018, **54**, 9623–9626.
90 J. Luo, R. Uprety, Y. Naro, C. Chou, D. P. Nguyen, J. W. Chin and A. Deiters, *J Am Chem Soc*, 2014, **136**, 15551–15558.
91 R. Schmidt, D. Geissler, V. Hagen and J. Bendig, *J. Phys. Chem. A*, 2005, **109**, 5000–5004.
92 B. Schade, V. Hagen, R. Schmidt, R. Herbrich, E. Krause, T. Eckardt and J. Bendig, *J. Org. Chem.*, 1999, **64**, 9109–9117.
93 Y. Fu and N. S. Finney, *RSC Adv.*, 2018, **8**, 29051–29061.
94 V. I. Martynov, A. A. Pakhomov, N. V. Popova, I. E. Deyev and A. G. Petrenko, *Acta Naturae*, 2016, **8**, 33–46.
95 M. D. Hammers, M. H. Hodny, T. K. Bader, M. M. Mahmoodi, S. Fang, A. D. Fenton, K. Nurie, H. O. Trial, F. Xu, A. T. Healy, Z. T. Ball, D. A. Blank and M. D. Distefano, *Org. Biomol. Chem.*, 2021, **19**, 2213–2223.
96 M. M. Mahmoodi, S. A. Fisher, R. Y. Tam, P. C. Goff, R. B. Anderson, J. E. Wissinger, D. A. Blank, M. S. Shoichet and M. D. Distefano, *Org. Biomol. Chem.*, 2016, **14**, 8289–8300.
97 J.-Y. Kang, D. Kawaguchi, I. Coin, Z. Xiang, D. D. M. O'Leary, P. A. Slesinger and L. Wang, *Neuron*, 2013, **80**, 358–370.
98 E. A. Lemke, D. Summerer, B. H. Geierstanger, S. M. Brittain and P. G. Schultz, *Nat. Chem. Biol.*, 2007, **3**, 769–772.
99 A. Deiters, D. Groff, Y. Ryu, J. Xie and P. G. Schultz, *Angew. Chem., Int. Ed.*, 2006, **45**, 2728–2731.
100 S. Tang, J.-Y. Cheng and J.-S. Zheng, *Tetrahedron Lett.*, 2015, **56**, 4582–4585.
101 S. Petersen, J. M. Alonso, A. Specht, P. Duodu, M. Goeldner and A. del Campo, *Angew. Chem. Int. Ed.*, 2008, **47**, 3192–3195.
102 A. Gandioso, M. Cano, A. Massaguer and V. Marchán, *J. Org. Chem.*, 2016, **81**, 11556–11564.
103 S. Tang, Z. Wan, Y. Gao, J.-S. Zheng, J. Wang, Y.-Y. Si, X. Chen, H. Qi, L. Liu and W. Liu, *Chem. Sci.*, 2016, **7**, 1891–1895.
104 E. Arbely, J. Torres-Kolbus, A. Deiters and J. W. Chin, *J. Am. Chem. Soc.*, 2012, **134**, 11912–11915.
105 P. W. R. Harris and M. A. Brimble, *Pept. Sci.*, 2013, **100**, 356–365.
106 R. Behrendt, P. White and J. Offer, *J. Pept. Sci.*, 2016, **22**, 4–27.
107 Y. Tatsu, Y. Shigeri, S. Sogabe, N. Yumoto and S. Yoshikawa, *Biochem. Biophys. Res. Commun.*, 1996, **227**, 688–693.
108 Y. Tatsu, Y. Shigeri, A. Ishida, K. Isamu, H. Fujisawa and N. Yumoto, *Bioorg. Med. Chem. Lett.*, 1999, **9**, 1093–1096.
109 R. Sreekumar, M. Ikebe, F. S. Fay and J. W. Walker, in *Methods in Enzymology*, Academic Press, 1998, vol. 291, pp. 78–94.
110 J. Hemphill, C. Chou, J. W. Chin and A. Deiters, *J. Am. Chem. Soc.*, 2013, **135**, 13433–13439.
111 Y. Tatsu, T. Nishigaki, A. Darszon and N. Yumoto, *FEBS Lett.*, 2002, **525**, 20–24.
112 Y. Li, C. A. Foss, D. D. Summerfield, J. J. Doyle, C. M. Torok, H. C. Dietz, M. G. Pomper and S. M. Yu, *Proc. Natl. Acad. Sci. U.S.A.*, 2012, **109**, 14767–14772.
113 C. Nadler, A. Nadler, C. Hansen and U. Diederichsen, *Eur. J. Org. Chem.*, 2015, **2015**, 3095–3102.
114 J. Hoffmann and U. Kazmaier, *Synthesis*, 2015, **47**, 411–420.
115 W. H. So and J. Xia, *Org. Lett.*, 2020, **22**, 214–218.
116 J. S. Wood, M. Koszelak, J. Liu and D. S. Lawrence, *J. Am. Chem. Soc.*, 1998, **120**, 7145–7146.
117 E. Janett, Y. Bernardinelli, D. Müller and C. G. Bochet, *Bioconjugate Chem.*, 2015, **26**, 2408–2418.
118 J. Ohata, M. B. Minus, M. E. Abernathy and Z. T. Ball, *J. Am. Chem. Soc.*, 2016, **138**, 7472–7475.
119 S. Chen, J. J. Yim and M. Bogyo, *Biol. Chem.*, 2020, **401**, 165–182.
120 A. Bianco, D. Kaiser and G. Jung, *J. Pept. Res.*, 1999, **54**, 544–548.
121 J. Luo, J. Torres-Kolbus, J. Liu and A. Deiters, *Chembiochem*, 2017, **18**, 1442–1447.
122 E. Ruoslahti, *Annu. Rev. Cell Dev. Biol.*, 1996, **12**, 697–715.
123 B. Jeschke, J. Meyer, A. Jonczyk, H. Kessler, P. Adamietz, N. M. Meenen, M. Kantlehner, C. Goepfert and B. Nies, *Biomaterials*, 2002, **23**, 3455–3463.
124 N. Huettner, T. R. Dargaville and A. Forget, *Trends Biotechnol.*, 2018, **36**, 372–383.
125 S. L. Bellis, *Biomaterials*, 2011, **32**, 4205–4210.
126 M. Alipour, M. Baneshi, S. Hosseinkhani, R. Mahmoudi, A. J. Arabzadeh, M. Akrami, J. Mehrzad and H. Bardania, *J. Biomed. Mater. Res. A*, 2020, **108**, 839–850.
127 C. A. Goubko, A. Basak, S. Majumdar, H. Jarrell, N. H. Khieu and X. Cao, *J. Biomed. Mater. Res. A*, 2013, **101A**, 787–796.
128 J. Auernheimer, C. Dahmen, U. Hersel, A. Bausch and H. Kessler, *J. Am. Chem. Soc.*, 2005, **127**, 16107–16110.
129 A. M. Porras Hernández, H. Pohlit, F. Sjögren, L. Shi, D. Ossipov, M. Antfolk and M. Tenje, *J. Mater. Sci.: Mater. Med.*, 2020, **31**, 89.
130 T. T. Lee, J. R. García, J. Paez, A. Singh, E. A. Phelps, S. Weis, Z. Shafiq, A. Shekaran, A. del Campo and A. J. García, *Nat Mater*, 2015, **14**, 352–360.
131 A. Specht, J.-S. Thomann, K. Alarcon, W. Wittayanan, D. Ogden, T. Furuta, Y. Kurakawa and M. Goeldner, *ChemBioChem*, 2006, **7**, 1690–1695.
132 J. M. Bergelson and M. E. Hemler, *Curr. Biol.*, 1995, **5**, 615–617.
133 B. Cheng, D. Shchepakin, M. P. Kavanaugh and D. Trauner, *ACS Chem. Neurosci.*, 2017, **8**, 1668–1672.
134 E. Vaselli, C. Fedele, S. Cavalli and P. A. Netti, *ChemPlusChem*, 2015, **80**, 1547–1555.
135 J. A. Frank, D. A. Yushchenko, D. J. Hodson, N. Lipstein, J. Nagpal, G. A. Rutter, J.-S. Rhee, A. Gottschalk, N. Brose, C. Schultz and D. Trauner, *Nat. Chem. Biol.*, 2016, **12**, 755–762.
136 J. Auernheimer, C. Dahmen, U. Hersel, A. Bausch and H. Kessler, *J. Am. Chem. Soc.*, 2005, **127**, 16107–16110.
137 M. M. Halassa, T. Fellin and P. G. Haydon, *Trends Mol. Med.*, 2007, **13**, 54–63.
138 H. Kettenmann and A. Verkhratsky, *Trends Neurosci.*, 2008, **31**, 653–659.
139 W.-S. Chung, N. J. Allen and C. Eroglu, *Cold Spring Harb. Perspect. Biol.*, 2015, **7**, a020370.
140 S. A. H. Hulgan, A. A. Jalan, I.-C. Li, D. R. Walker, M. D. Miller, A. J. Kosgei, W. Xu, G. N. Phillips and J. D. Hartgerink, *Biomacromolecules*, 2020, **21**, 3772–3781.
141 L. E. R. O'Leary, J. A. Fallas, E. L. Bakota, M. K. Kang and J. D. Hartgerink, *Nat. Chem.*, 2011, **3**, 821–828.
142 A. A. Jalan, D. Sammon, J. D. Hartgerink, P. Brear, K. Stott, S. W. Hamaia, E. J. Hunter, D. R. Walker, B. Leitinger and R. W. Farndale, *Nat. Chem. Biol.*, 2020, **16**, 423–429.
143 J. L. Zitnay, Y. Li, Z. Qin, B. H. San, B. Depalle, S. P. Reese, M. J. Buehler, S. M. Yu and J. A. Weiss, *Nat. Commun.*, 2017, **8**, 14913.
144 M. I. Converse, R. G. Walther, J. T. Ingram, Y. Li, S. M. Yu and K. L. Monson, *Acta Biomaterialia*, 2018, **67**, 307–318.
145 K. A. Clements, A. M. Acevedo-Jake, D. R. Walker and J. D. Hartgerink, *Biomacromolecules*, 2017, **18**, 617–624.
146 D. R. Walker, S. A. H. Hulgan, C. M. Peterson, I.-C. Li, K. J. Gonzalez and J. D. Hartgerink, *Nat. Chem.*, 2021, **13**, 260–269.

147 A. J. de Graaf, M. Kooijman, W. E. Hennink and E. Mastrobattista, *Bioconjugate Chem.*, 2009, **20**, 1281–1295.
148 C. C. Liu and P. G. Schultz, *Annu. Rev. Biochem.*, 2010, **79**, 413–444.
149 A. S. Baker and A. Deiters, *ACS Chem. Biol.*, 2014, **9**, 1398–1407.
150 A. R. Nödling, L. A. Spear, T. L. Williams, L. Y. P. Luk and Y.-H. Tsai, *Essays Biochem*, 2019, **63**, 237–266.
151 W. Gao, E. Cho, Y. Liu and Y. Lu, *Front. Pharmacol.*, 2019, **10**, 611.
152 I. Drienovská and G. Roelfes, *Nat. Catal.*, 2020, **3**, 193–202.
153 S. Zhao, J. Shi, G. Yu, D. Li, M. Wang, C. Yuan, H. Zhou, A. Parizadeh, Z. Li, M.-X. Guan and S. Ye, *Commun Biol*, 2020, **3**, 1–11.
154 J. Wang, Y. Liu, Y. Liu, S. Zheng, X. Wang, J. Zhao, F. Yang, G. Zhang, C. Wang and P. R. Chen, *Nature*, 2019, **569**, 509–513.
155 M. S. Padilla, C. A. Farley, L. E. Chatkewitz and D. D. Young, *Tetrahedron Lett.*, 2016, **57**, 4709–4712.
156 S. Zhu, M. Riou, C. A. Yao, S. Carvalho, P. C. Rodriguez, O. Bensaude, P. Paoletti and S. Ye, *Proc. Natl. Acad. Sci. U.S.A.*, 2014, **111**, 6081–6086.
157 A. S. Larson and P. J. Hergenrother, *Biochemistry*, 2014, **53**, 188–201.
158 D. S. Miller, S. Chirayil, H. L. Ball and K. J. Luebke, *ChemBioChem*, 2009, **10**, 577–584.
159 D. M. Rothman, E. J. Petersson, M. E. Vázquez, G. S. Brandt, D. A. Dougherty and B. Imperiali, *J. Am. Chem. Soc.*, 2005, **127**, 846–847.
160 Y. Tong, G. S. Brandt, M. Li, G. Shapovalov, E. Slimko, A. Karschin, D. A. Dougherty and H. A. Lester, *Am. J. Physiol. Cell Physiol.*, 2001, **117**, 103–118.
161 K. D. Philipson, J. P. Gallivan, G. S. Brandt, D. A. Dougherty and H. A. Lester, *Am. J. Physiol. Cell Physiol.*, 2001, **281**, C195–C206.
162 M. W. Nowak, P. C. Kearney, J. R. Sampson, M. E. Saks, C. G. Labarca, S. K. Silverman, W. Zhong, J. Thorson, J. N. Abelson, N. Davidson, P. G. Schultz, D. A. Dougherty and H. A. Lester, *Science*, 1995, **268**, 439–442.
163 M. W. Nowak, J. P. Gallivan, S. K. Silverman, C. G. Labarca, D. A. Dougherty and H. A. Lester, in *Methods in Enzymology*, Academic Press, 1998, vol. 293, pp. 504–529.
164 M. E. Saks, J. R. Sampson, M. W. Nowak, P. C. Kearney, F. Du, J. N. Abelson, H. A. Lester and D. A. Dougherty, *J. Biol. Chem.*, 1996, **271**, 23169–23175.
165 R. Rakauskaitė, G. Urbanavičiūtė, A. Rukšėnaitė, Z. Liutkevičiūtė, R. Juškėnas, V. Masevičius and S. Klimašauskas, *Chem. Commun.*, 2015, **51**, 8245–8248.
166 C. Chou, D. D. Young and A. Deiters, *Chembiochem*, 2010, **11**, 972–977.
167 R. Uprety, J. Luo, J. Liu, Y. Naro, S. Samanta and A. Deiters, *ChemBioChem*, 2014, **15**, 1793–1799.
168 W. E. Georgianna, H. Lusic, A. L. McIver and A. Deiters, *Bioconjugate Chem.*, 2010, **21**, 1404–1407.
169 H.-M. Lee, W. Xu and D. S. Lawrence, *J. Am. Chem. Soc.*, 2011, **133**, 2331–2333.
170 M. Ghosh, I. Ichetovkin, X. Song, J. S. Condeelis and D. S. Lawrence, *J. Am. Chem. Soc.*, 2002, **124**, 2440–2441.
171 M. Ghosh, X. Song, G. Mouneimne, M. Sidani, D. S. Lawrence and J. S. Condeelis, *Science*, 2004, **304**, 743–746.
172 M. A. Priestman and D. S. Lawrence, *Biochim. Biophys. Acta, Proteins Proteom.*, 2010, **1804**, 547–558.
173 K. Zou, S. Cheley, R. S. Givens and H. Bayley, *J. Am. Chem. Soc.*, 2002, **124**, 8220–8229.
174 Y.-B. Kim, S. Choi, M.-C. Choi, M.-A. Oh, S.-A. Lee, M. Cho, K. Mizuno, S.-H. Kim and J. W. Lee, *J. Biol. Chem.*, 2008, **283**, 10089–10096.
175 P. Cohen, *Eur. J. Biochem.*, 2001, **268**, 5001–5010.
176 J. Neddens, M. Temmel, S. Flunkert, B. Kerschbaumer, C. Hoeller, T. Loeffler, V. Niederkofler, G. Daum, J. Attems and B. Hutter-Paier, *Acta Neuropathol. Commun.*, 2018, **6**, 52.
177 M. Perluigi, E. Barone, F. Di Domenico and D. A. Butterfield, *Biochim. Biophys. Acta, Mol. Basis Dis.*, 2016, **1862**, 1871–1882.
178 I. Wiesauer, C. Gaumannmüller, I. Steinparzer, B. Strobl and P. Kovarik, *Mol Cell Biol*, 2015, **35**, 716–727.
179 N. P. Ferenz, A. Gable and P. Wadsworth, *Semin. Cell Dev. Biol.*, 2010, **21**, 255–259.
180 Q. Kuang, P. Purhonen and H. Hebert, *Cell. Mol. Life Sci.*, 2015, **72**, 3677–3693.
181 M. Cheriyan, C. S. Pedamallu, K. Tori and F. Perler, *J. Biol. Chem.*, 2013, **288**, 6202–6211.
182 S. Ellilä, J. M. Jurvansuu and H. Iwaï, *FEBS Lett.*, 2011, **585**, 3471–3477.
183 J. Seong, S. Lu, M. Ouyang, H. Huang, J. Zhang, M. C. Frame and Y. Wang, *Chem. Biol.*, 2009, **16**, 48–57.
184 B. D. Ventura and H. D. Mootz, *Biol. Chem.*, 2019, **400**, 467–475.
185 A. R. Raghavan, K. Salim and V. G. Yadav, *ACS Synth. Biol.*, 2020, **9**, 2291–2300.
186 C. C. Goodnow, J. Crosbie, S. Adelstein, T. B. Lavoie, S. J. Smith-Gill, R. A. Brink, H. Pritchard-Briscoe, J. S. Wotherspoon, R. H. Loblay, K. Raphael, R. J. Trent and A. Basten, *Nature*, 1988, **334**, 676.